

Chapter 3

Modular Nucleic Acid Assembled p/MHC Microarrays for Multiplexed Sorting of Antigen- Specific T Cells

2.1 Introduction

T cells constitute an important part of the acquired immune system. They recognize a diversity of antigens through the highly variable, hetero-dimeric T cell receptor protein (TCR), with approximately 10^7 different antigen specificities (1). The initiation of the T cell immune response is triggered by the engagement of the TCR with processed antigenic peptides (e.g. from a bacterial pathogen) that are bound to Major Histocompatibility Complex (p/MHC) molecules presented on the surface of antigen presenting cells (APCs), leading to downstream T cell proliferation and maturation into effector populations. After pathogen clearance, a subset of the activated T cells transition into memory cells, providing the immune system with the capacity for rapid response

towards previously encountered pathogens. As a consequence, an individual's collection of T cells and their antigen specificities, collectively called the T cell repertoire, is an evolving, extensive repository of cellular immune responses against self and foreign antigens. It is of fundamental and therapeutic importance to detect and survey these T cell populations.

The development of soluble p/MHC tetramers for labeling antigen-specific T cells has enabled the direct phenotypic analysis of antigen-specific T cell populations with flow cytometry (2). Conventionally, p/MHC tetramers are prepared by mixing enzymatically biotinylated p/MHC molecules with preparations of streptavidin (SA)-fluorophore conjugates. While p/MHC monomers have low affinities (2, 3), their tetramer counterparts exhibit much higher avidity, permitting T cell detection via flow cytometry to become a standard assay. However, because p/MHC tetramer-stained T cell populations are encoded optically (i.e. one unique fluorophore required per p/MHC specificity), the number of antigen-specificities that can be interrogated simultaneously within a population is limited by spectral overlap. In addition, serial flow cytometry detection of distinct antigen-specific T cells is generally restricted by sample size. Efforts to increase the degree of multiplexing generally revolve around polychromatic flow cytometry utilizing quantum dots (4, 5). However, cost, sample preparation time, and color compensation complexity also increase correspondingly.

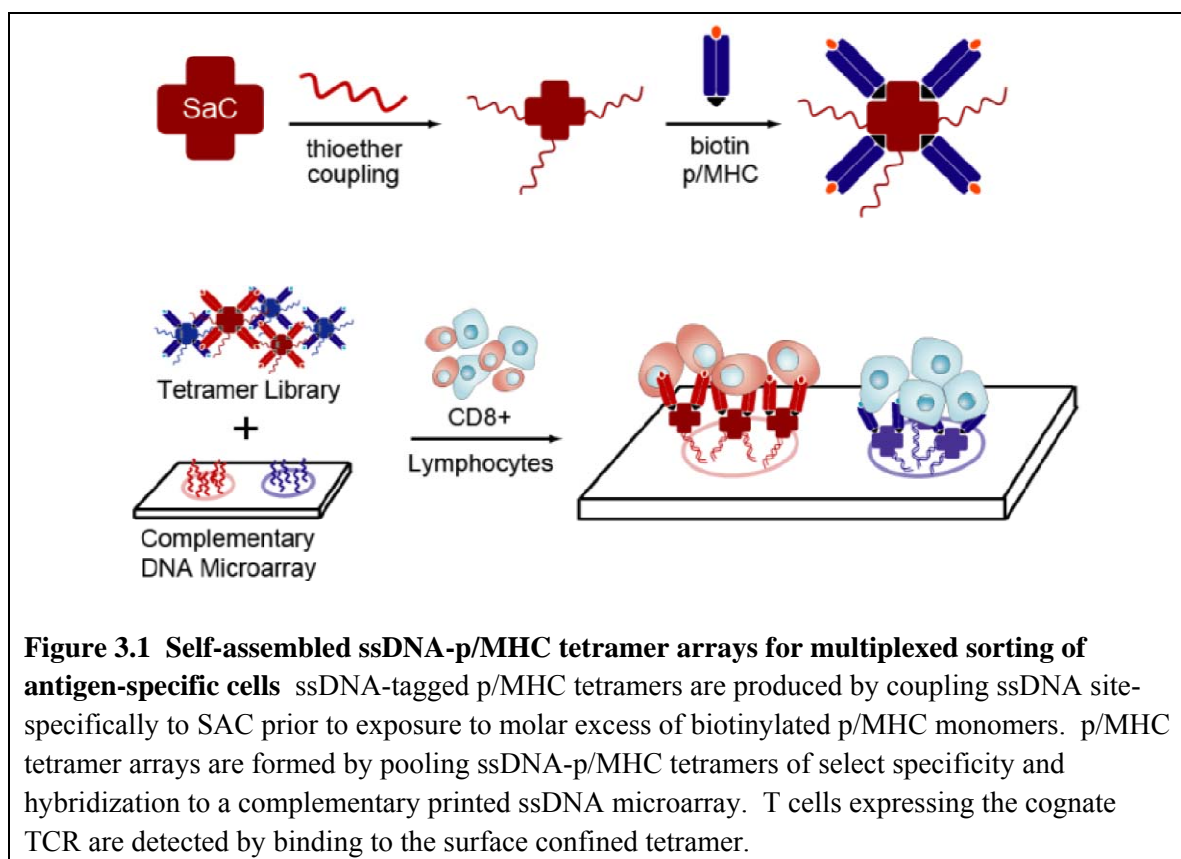
As an alternative to flow cytometry, several groups have reported microarray-based T cell detection schemes, in which collections of p/MHC complexes are printed on a supporting substrate (6–9). A population of cells is applied directly to the p/MHC array where target antigen-specific T cells bind to regions spotted with the cognate p/MHC and

are detected optically. Analogous to DNA and protein microarrays, the readout of such assays is dependent on location rather than distinct fluorescent signals, thus potentially increasing the degree of multiplexing.

A factor that needs to be addressed before p/MHC arrays are used for broader studies and applications concerns the reproducibility and robustness of p/MHC arrays produced by spotting onto treated and/or derivatized surfaces. Ideally p/MHC complexes should be immobilized such that their functional conformations are preserved. Analogous protein arrays produced via antibody adsorption to unmodified and derivatized surfaces can suffer from surface induced effects including protein denaturation and protein adsorption in inactive orientations (10–12). To circumvent such problems, customized surfaces and relatively mild chemistries for protein immobilization have been developed (13–18). However, often the surface that meets the demands of the application requires a high level of technical expertise and/or is limited in accessibility (19).

We report here on the method of Nucleic Acid Cell Sorting (NACS), which is based upon the design and application of nucleic acid assembled p/MHC tetramer arrays for multiplexed sorting of antigen-specific T cells. For NACS, p/MHC tetramers of distinct specificities are conjugated to unique sequences of ssDNA in a site-specific fashion. A collection of ssDNA-tagged p/MHC complexes is then self-assembled by DNA hybridization onto a glass slide printed with the complementary DNA sequences. Fully assembled p/MHC tetramer arrays are used to sort mixed populations of antigen-specific T cells (**Figure 3.1**). This strategy of using DNA pendants as molecular linkages (20-25) is simple and highly modular. Most importantly, T cell array binding is

optimized by utilizing cysteine-engineered streptavidin (SAC) for ssDNA-p/MHC tetramer production, resulting in NACS p/MHC arrays that outperform conventional spotted arrays assessed by performance criteria such as reproducibility and homogeneity. The versatility of using DNA tags is also exploited to enable selective detachment of T cells with restriction endonucleases. Demonstrative experiments regarding NACS sensitivity, multiplexing and limit of detection are performed with cell lines and finally with T cells isolated from cancer patients.



3.2 Experimental Methods

3.2.1 Microarray Fabrication

All DNA strands were purchased from IDT with HPLC purification. DNA microarrays were printed by the microarray facility at the Institute for Systems Biology (ISB—Seattle, WA) on amine-coated glass slides (GAPS II, Corning) in identical triplicate 12x12 arrays containing alternative rows of A, B and C spots, or A_{EcoRI} and B_{BamHI} with a SMPXB15 pin (Arrayit). Sequences for all strands can be found at **Table 3.1**.

Table 3.1 Orthogonal DNA sequences for spatial encoding of p/MHC tetramers

Name	Sequence*
A	5' - AAA AAA AAA AAA AAT CCT GGA GCT AAG TCC GTA AAA AAA AAA AAT CCT GGA GCT AAG TCC GTA AAA AAA AAA AAA A
A'	5' - NH ₂ - AAA AAA AAA ATA CGG ACT TAG CTC CAG GAT
B	5' - AAA AAA AAA AAA AGC CTC ATT GAA TCA TGC CTA AAA AAA AAA AGC CTC ATT GAA TCA TGC CTA AAA AAA AAA AAA A
B'	5' - NH ₂ - AAA AAA AAA ATA GGC ATG ATT CAA TGA GGC
C	5' - AAA AAA AAA AAA AGC ACT CGT CTA CTA TCG CTA AAA AAA AAA AGC ACT CGT CTA CTA TCG CTA AAA AAA AAA AAA A
C'	5' - NH ₂ - AAA AAA AAA ATA GCG ATA GTA GAC GAG TGC
A _{EcoRI}	5' - AAA AAA AAA AAA GAG CTA AGT CCG TAG AAT TCA AAA AAA AAA GAG CTA AGT CCG TAG AAT TCA AAA AAA AAA AAA
A _{EcoRI} '	5' - NH ₂ - AAA AAA AAA AGA ATT CTA CGG ACT TAG CTC CAG GAT
B _{BamHI}	5' - AAA AAA AAA AAA TTG AAT CAT GCC TAG GAT CCA AAA AAA AAA TTG AAT CAT GCC TAG GAT CCA AAA AAA AAA AAA
B _{BamHI} '	5'- NH ₂ - AAA AAA AAA AGG ATC CTA GGC ATG ATT CAA TGA GGC

* All sequences to be conjugated to SAC (A', B', C', A_{EcoRI}', and B_{BamHI}') were designed with a polyA linker followed by a 20mer hybridization region. The 5' amine is required for the attachment of the hetero-bifunctional maleimide derivative MHPH. Sequences printed on glass substrates (A, B, C, A_{EcoRI}, and B_{BamHI}) were designed with two hybridization regions separated by polyAs. This was designed to facilitate electrostatic adsorption to amine glass substrates.

3.2.2 Production of ssDNA-SAC conjugates

The pET-3a plasmid containing the SAC gene was a kind gift from Takeshi Sano (Harvard Medical School). The expression of SAC was performed according to previously published protocols (26). Briefly, transformed BL21(DE3)-pLysE cells were grown at 37°C with shaking in LB medium and selection antibiotics ampicillin and chlorophenicol. The cells were induced at OD₆₀₀ = 0.6 with IPTG and kept spinning for another 4 hours. The culture was then centrifuged at 1600g for 10 min and lysed with lysis buffer (2 mM EDTA, 30 mM Tris-HCl, 0.1% Triton X-100, pH 8.0). The insoluble inclusion bodies were then separated from the lysate by centrifugation at 39,000g for 15 min and dissolved in 6 M guanidine-HCl, pH 1.5 to the original culture volume. The SAC lysate was then refolded by dialysis in 0.2 M Sodium acetate, 10 mM β-mercaptoethanol (β-ME) pH 6.0 overnight before dialyzed against 50mM Sodium bicarbonate, 500 mM NaCl, 10 mM β-ME pH 11 in preparation for column purification. Refolded volumes of SAC were mixed 1:1 with binding buffer (50 mM Sodium bicarbonate, 500 mM NaCl, 10mM β-ME, pH 11). A gravity column packed with 1.5 ml of iminobiotin agarose resin (Pierce) was washed with 10 ml of binding buffer. The refolded mixture was then applied to the column and the eluted fractions were collected and reapplied to the column again, to maximize SAC recovery. After washing the

column with 20 ml binding buffer, SAC was eluted with pH 4 elution buffer (50 mM Sodium acetate, 10mM β -ME). Fractions containing SAC, as monitored by OD280, were collected, buffer exchanged to PBS containing 10 mM β -ME, and concentrated to 1 mg/ml final concentration using 10K mwco filters (Millipore). Immediately prior to conjugation, stock SAC was buffer exchanged to PBS containing 5mM Tris(2-Carboxyethyl) phosphine Hydrochloride (TCEP) using zeba desalting columns (Pierce). MHPH (3-N-Maleimido-6-hydraziniumpyridine hydrochloride, Solulink) in DMF was added to SAC at a molar excess of 300:1. In parallel, SFB in DMF (succinimidyl 4-formylbenzoate, Solulink) was added in a 40:1 molar excess to 5'aminated oligos. The mixtures were reacted at room temperature (RT) for 3–4 hours before buffer exchanged to citrate (50mM sodium citrate, 150 mM NaCl, pH 6.0) using zeba columns. The SFB-labeled oligos were combined in a 20:1 molar excess with the derivatized SAC and incubated overnight at RT. Unreacted oligos were removed using a Pharmacia Superdex 200 gel filtration column at 0.5 ml/min isocratic flow of PBS. Fractions containing the SAC-oligo conjugates were concentrated using 10K mwco concentration filters (Millipore).

3.2.3 Preparation of T cells

The cDNA from the alpha and beta chains of a TCR specific for tyrosinase368-376 was a kind gift from Michael I. Nishimura (Medical University of South Carolina, Charleston, SC). The alpha and beta chains were cloned into a lentiviral vector where both transgenes were linked by a 2A self-cleaving sequence as described (27). Concentrated supernatant from this lentiviral vector was used to infect Jurkat cells to generate Jurkat ^{α -Tyro} cells. The MSGV1-F5Aft2AB retroviral vector expressing the F5

MART-1 TCR was a kind gift from Steven A. Rosenberg and Richard Morgan (Surgery Branch, National Cancer Institute Bethesda, MD). The MSGV1-F5AfT2AB retroviral supernatant was used to infect Jurkat cells to generate the Jurkat^{α-MART-1} cell line. The Jurkat^{α-NY-ESO-1} cell line was a generous gift from Robert Prins (UCLA). To generate primary human T cell cultures expressing the F5 MART-1 TCR, PBMCs obtained from leukapheresis were activated for 48 hours with 50 ng/ml of OKT3 (muromonab anti-human CD3 antibody, Ortho-Biotech, Bridgewater, NJ) and 300 U/ml of IL-2 (adesleukin, Novartis, Emeryville, CA). MSGV1-F5AfT2AB retrovirus supernatant was applied to retronectin-coated wells (Takara Bio Inc., Japan). Then activated PBMC in RPMI plus 5% human AB serum supplemented by 300 IU of IL-2 were added to these wells and incubated at 37°C overnight at 5% CO₂. On the following day, PBMC are transferred to a second set of pre-coated retronectin retroviral vector tissue culture plates and incubated at 37°C overnight at 5% CO₂. Cells were subsequently washed and re-suspended in culture media described above. Frozen leukapheresis fractions from patients NRA11, NRA 13 (UCLA IRB#03-12-023) and F5-1 (UCLA IRB #08-02-020-02A) were thawed and incubated overnight in RPMI supplemented with 10% human AB serum and 1% penicillin, streptomycin, and amphotericin (Omega Scientific). F5-1 cells were used immediately following incubation. NRA11 and NRA13 samples were CD8⁺ enriched (anti-CD8 microbeads, Miltenyi Biotech) using an AutoMACS machine according to the manufacturer's instructions. Following separation, the cells were kept at in RPMI-humanAB media containing 30 U IL2/mL.

3.2.4 T Cell Sorting Methods

The HLA-A*0201 restricted MHC class I monomers loaded with tyrosinase₃₆₉₋₃₇₇ (YMDGTMSQV), MART-1₂₆₋₃₅ (ELAGIGILTV) and NY-ESO-1157-165 (SLLMWITQC) were produced in house according to previous published protocols (28). A2.1-restricted EBV BMLF1₂₅₉₋₂₆₇ (GLCTLVAML), CMV pp65₄₉₅₋₅₀₃ (NLVPMVATV), murine H-2Kb/-OVA₂₅₇₋₂₆₄ (SIINFEKL), and murine H-2Db/-gp100₂₅₋₃₃ (KVPRNQDWL) as well as all fluorescent HLA-A*0201 tetramers were purchased from Beckman Coulter. Lipophilic cell membrane staining dyes DiO, DiD, and DiL were purchased from Invitrogen.

Prior to experiments, microarray slides were blocked to prevent non-specific cell binding with 1 mg/ml PEG-NHS ester (Sunbio) in PBS for 2 hours at RT. Four-fold molar excess of p/MHC monomers were combined with ssDNA-SAC at 37°C for 20 min. ssDNA-p/MHC tetramers were hybridized to DNA arrays for 1 hour at 37°C in 200 µl media and rinsed with 3% FBS in PBS. T cells (10⁶ /100 µl media) were incubated on the array at 37°C for 30 min. The arrays were rinsed with 3% FBS in PBS and cell capture visualized via brightfield (Nikon Eclipse TE2000) and/or confocal microscopy (Nikon E800). Post T cell capture p/MHC tetramer staining was done by incubating the array with 200 µl of media containing fluorescent p/MHC tetramer along with fluorescent cDNA (Cy5-A' and/or Cy3-B'). The arrays were rinsed with 3% FBS in PBS prior to imaging. For selective T cell release experiments, three identical arrays were used to immobilize cells. Treatment with EcoRI, BamHI, or DNase was in RPMI media for 1–2 hours at 37°C. DNase was purchased from Sigma, all other enzymes from NEbiolabs.

For p/MHC comparative studies, SuperEpoxy and SuperProtein (representing covalent and hydrophobic surfaces respectively) were purchased from Arrayit (Sunnyvale, CA). Amine GAPS II slides (electrostatic) were purchased from Corning. Polycarboxylate hydrogel (hydrophilic) slides were purchased from XanTec (Germany). Fluorescent MART-1 tetramers were printed according to manufacturer's instructions for each slide. Cell sorting images were quantified with ImageJ (NIH) and fitted to the Hill Function (NACS n=2, R2=0.95, Covalent n=2.1, R2 =0.97) with Origin (OriginLab, MA).

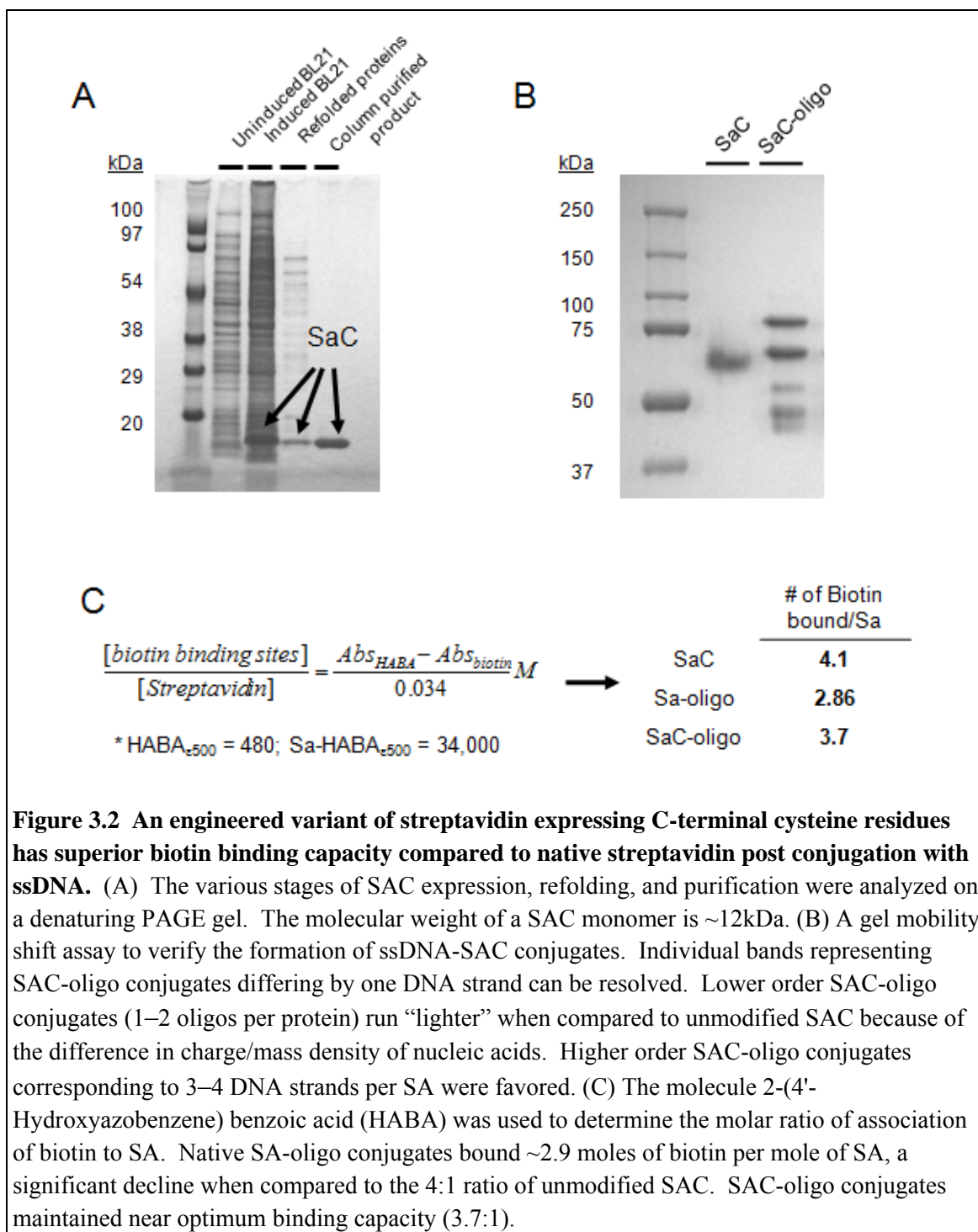
3.3 Results and Discussion

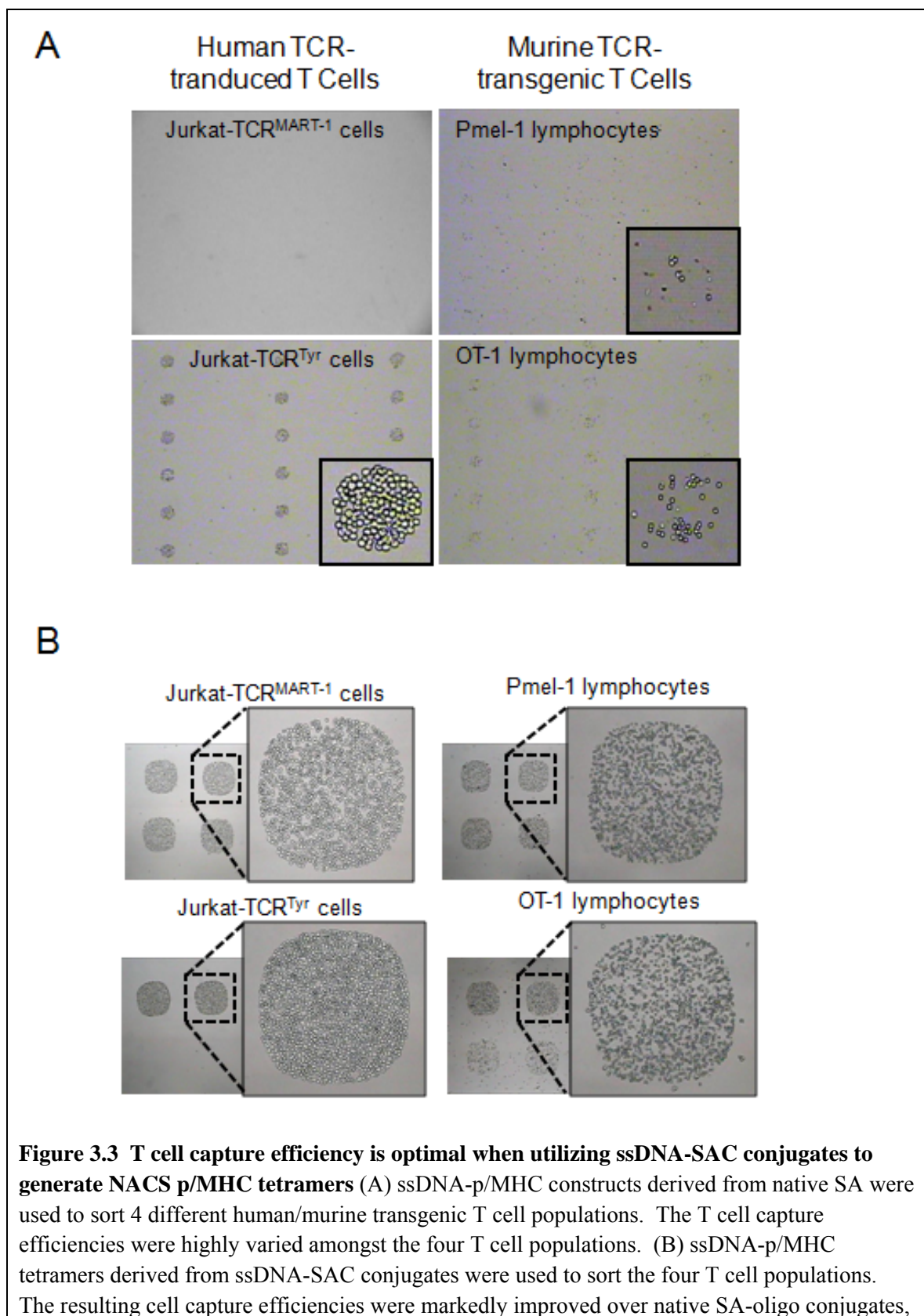
3.3.1 Rational design of ssDNA-encoded p/MHC tetramers

The standard scaffold most frequently used to assemble p/MHC monomers into tetramers is SA-phycoobiliprotein (using the protein fluorophores phycoerythrin (PE) or allophycocyanin (APC)) conjugates. Because SA-phycoobiliprotein conjugates are produced via chemical cross-linking, most functional groups are exhausted and/or modified, prohibiting the conjugation of ssDNA. In addition, the attachment of molecular fluorophores to native SA reduces the binding capacity for biotin, an effect attributed to the modification of lysine121 that occurs with amide coupling strategies. This residue is in close proximity to the ligand binding pockets (29, 30). To circumvent this, Altman and co-workers (29) employed a recombinant mutant of SA for fluorescent p/MHC tetramer preparations. This variant incorporates a cysteine residue at the carboxy-terminus (31), a site removed from the biotin binding pocket. The conjugation

of cysteine-reactive maleimide derivatives is restricted to the C-terminus because cysteine residues are absent in native SA.

We expressed SAC, coupled the protein with 5'-maleimide ssDNA, and verified the formation of conjugates with mobility shift assays (**Figure 3.2**). In parallel, ssDNA was coupled to native SA for direct comparison. To test biotin binding capacity, SAC-oligo conjugates were probed with 2-(4'-Hydroxyazobenzene) benzoic acid (HABA) (32), a molecular mimic of biotin with distinct optical density coefficients dependent on whether biotin is bound to SA or not. A biotin:SA molar ratio of association significantly below 4 in the assay would indicate a reduction in biotin binding capacity. Conjugates derived from native SA were greater than one full unit below the expected value (2.86 versus 4.0), while conjugates formed with SAC maintained near optimal (3.7) binding capacity (**Figure 3.2C**). These conjugates were then tested across 4 different monoclonal T cell populations (2 human TCR-transduced cell lines and 2 murine TCR-transgenic splenocyte cell suspensions). ssDNA-tagged SAC constructs had markedly higher cell capture efficiencies (**Figure 3.3B**) when compared with p/MHC tetramers prepared with native SA (**Figure 3.3A**). All subsequent NACS tetramers were prepared with the SAC variant.

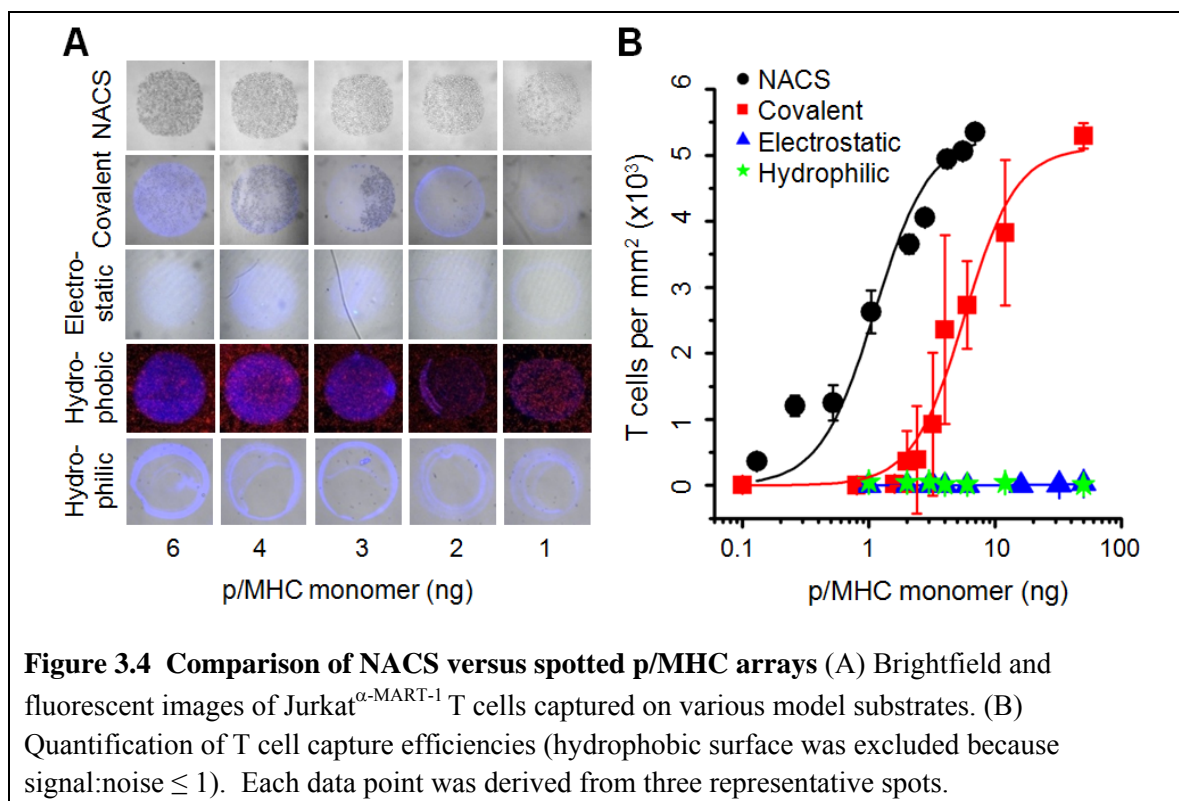




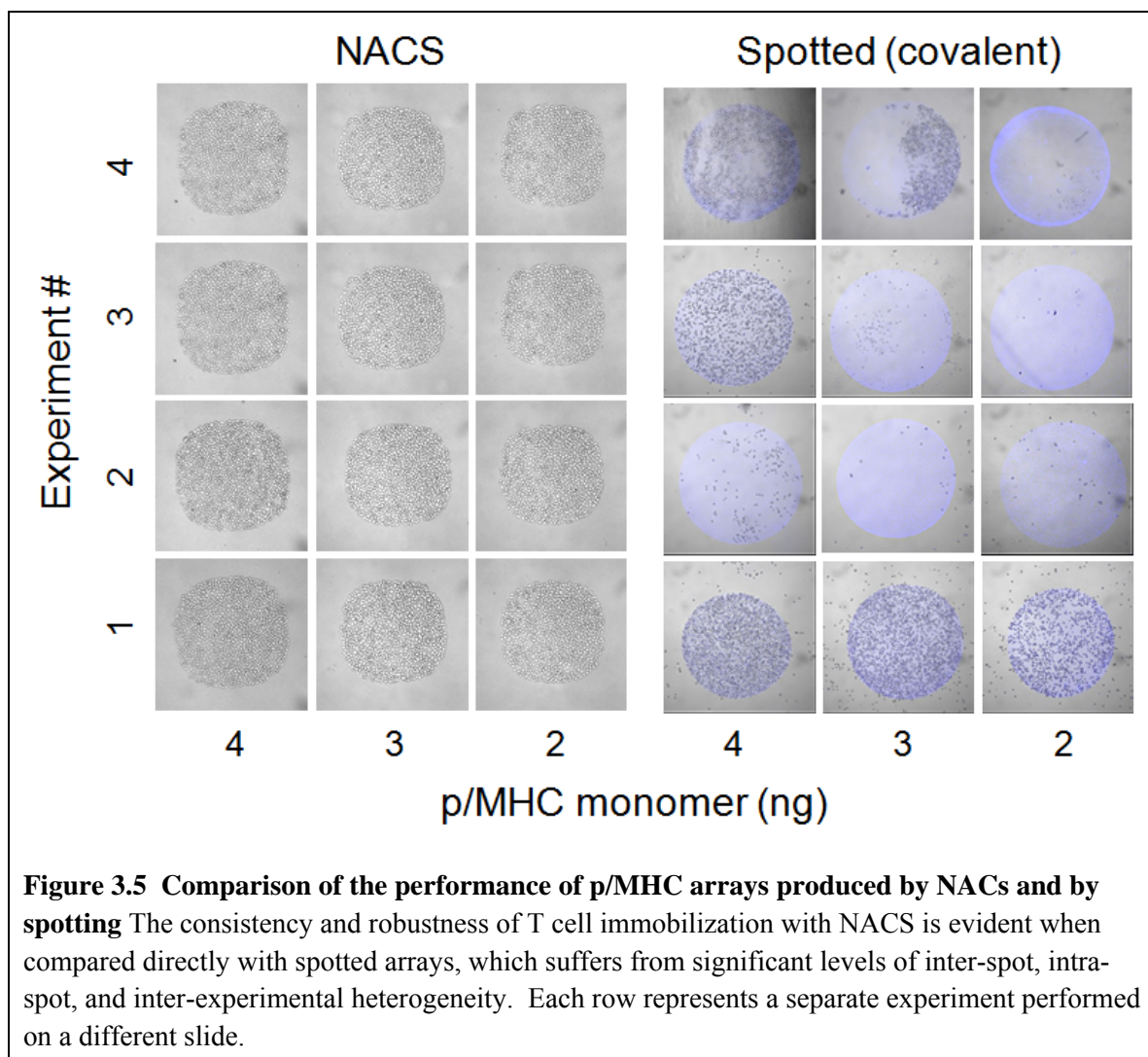
demonstrating that SAC is necessary for the production of high affinity ssDNA-p/MHC tetramers.

3.3.2 Performance of p/MHC arrays produced via DNA immobilization and direct spotting

We directly compared the performance of NACS with conventional direct spotting strategies on various model substrates. The substrates were selected to represent the spectrum of surface chemistries typically used to immobilize proteins (covalent, electrostatic, hydrophobic, and hydrophilic adsorption). Serial dilutions of a fluorescent p/MHC tetramer, MART-1, were spotted on the substrates according to manufacturer's instructions. Jurkat^{α-MART-1} T cells (the human T leukemia cell line Jurkat transduced with the F5 MART-1 TCR (**33**) specific for MART-1) were applied to the array and representative images collected (**Figure 3.4A**) and quantified (**Figure 3.4B**). We observed little to no T cell capture (electrostatic, hydrophilic) or significant noise (hydrophobic) on the majority of the surfaces investigated compared to NACS arrays immobilized with identical concentrations of p/MHC tetramers. T cell binding was observed on one surface (covalent) but cell capture was highly variable as evidenced by both intra-spot and inter-spot heterogeneity and cross experimental variation (**Figure 3.5**). Moreover, to achieve equivalent T cell capture densities, NACS p/MHC arrays required >5 times less material than covalent immobilization. (p/MHC monomer at half max $\equiv K_{1/2} = 1.1$ ng for NACS and 5.7 ng for covalent immobilization).



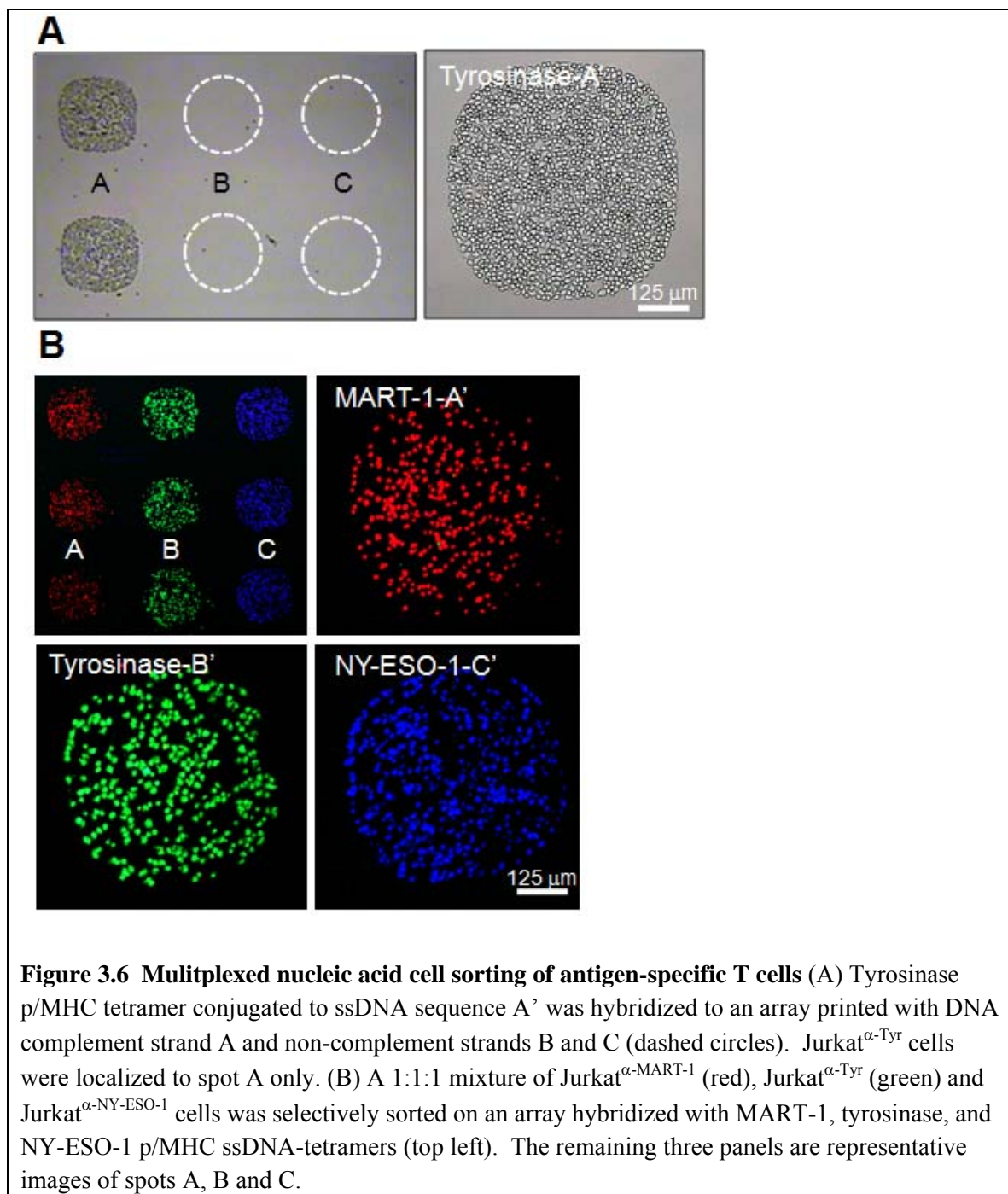
The performance and reproducibility of NACS p/MHC arrays is markedly improved and represents an integral step towards expanding array-based T cell detection schemes for broader applications. This likely has a few causes. First, surface-tethered ssDNA-p/MHC tetramers may enjoy greater orientational freedom at the surface/solution interface compared with adsorbed proteins which are required to conform to the surface. This effect may increase the density of functional protein and consequently reduce the amount of material required for array production. Second, the hydration state of the environment during the production and subsequent storage of protein arrays is an important factor for array reproducibility (10, 13, 18). This effect is minimized with NACS because DNA chips can be printed and stored dry for extended periods of time and ssDNA-tagged p/MHC tetramer arrays are self-assembled in solution immediately prior to an experiment.



3.3.3 NACS specificity and limit of detection

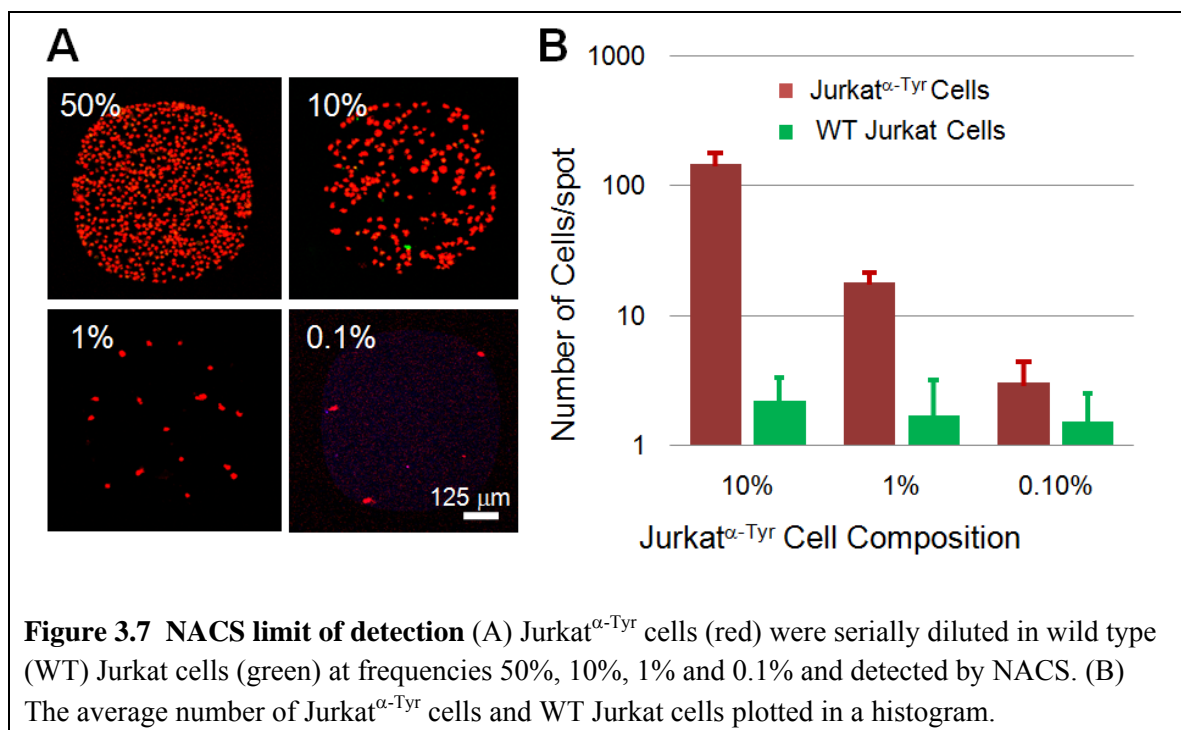
To evaluate the specificity of p/MHC array assembly and T cell sorting, a ssDNA-p/MHC tetramer, tyrosinase, with pendant DNA sequence A' was hybridized to a DNA microarray printed with the complementary strand (A) along with two additional distinct sequences (designated B and C). A homogeneous population of Jurkat ^{α -Tyr} cells (Jurkat cells transduced with a TCR specific for tyrosinase) (34) was then applied to the array. Jurkat ^{α -Tyr} T cells localized to the complementary spots (A) containing the hybridized

cognate p/MHC but not to spots printed with the non-complementary sequences B and C (**Figure 3.6A**). The mean binding capacity calculated from three spots ($\sim 600 \mu\text{m}$) was $\sim 1486 \pm 62$ Jurkat ^{α -Tyr} T cells.



To illustrate the multiplexing capability of NACS, MART-1, tyrosinase, and NY-ESO-1 ssDNA-p/MHC tetramers encoded to DNA sequences A, B and C respectively were combined and assembled simultaneously to a three element DNA microarray (strands A, B, and C). A 1:1:1 mixed population of Jurkat^{α-MART-1}, Jurkat^{α-Tyr} and Jurkat^{α-NY-ESO-1} (Jurkat human T cells transduced with the TCR (35) specific for NY-ESO-1) cells prestained with lipophilic dyes (red, green and blue respectively) was applied to the array and localized into alternating columns (**Figure 3.6B**). Minimal cross-reactivity was observed. The average density of spots was about a factor of three less than homogeneous sorting (440 ± 28 T cells/spot).

To determine the limit of detection, target populations of Jurkat^{α-Tyr} cells were spiked in at 10%, 1% and 0.1% into wild type (w.t.) Jurkat cells and sorted (**Figure 3.7**). The T cell capture density per spot per species for each mixture was enumerated and averaged (right panel). The number of non-specific w.t. Jurkat cells that adhered to the array was constant throughout all dilutions while the number of Jurkat^{α-Tyr} T cells captured per spot decreased linearly in relation to the fractional composition of Jurkat^{α-Tyr} cells with a detection limit that was ~ 1 in 1000 cells—a limit that corresponds well to the total number of cells that can be captured per spot. Thus, the sensitivity of this approach is strictly a geometric constraint since antigen-specific T cells that settle on inert areas cannot sample and bind to their cognate p/MHC tetramer. The sensitivity can be improved by increasing the size of the capture region (i.e. increase spot diameter and/or incorporate spot redundancy) or by reducing inert regions (i.e. increase printing density).



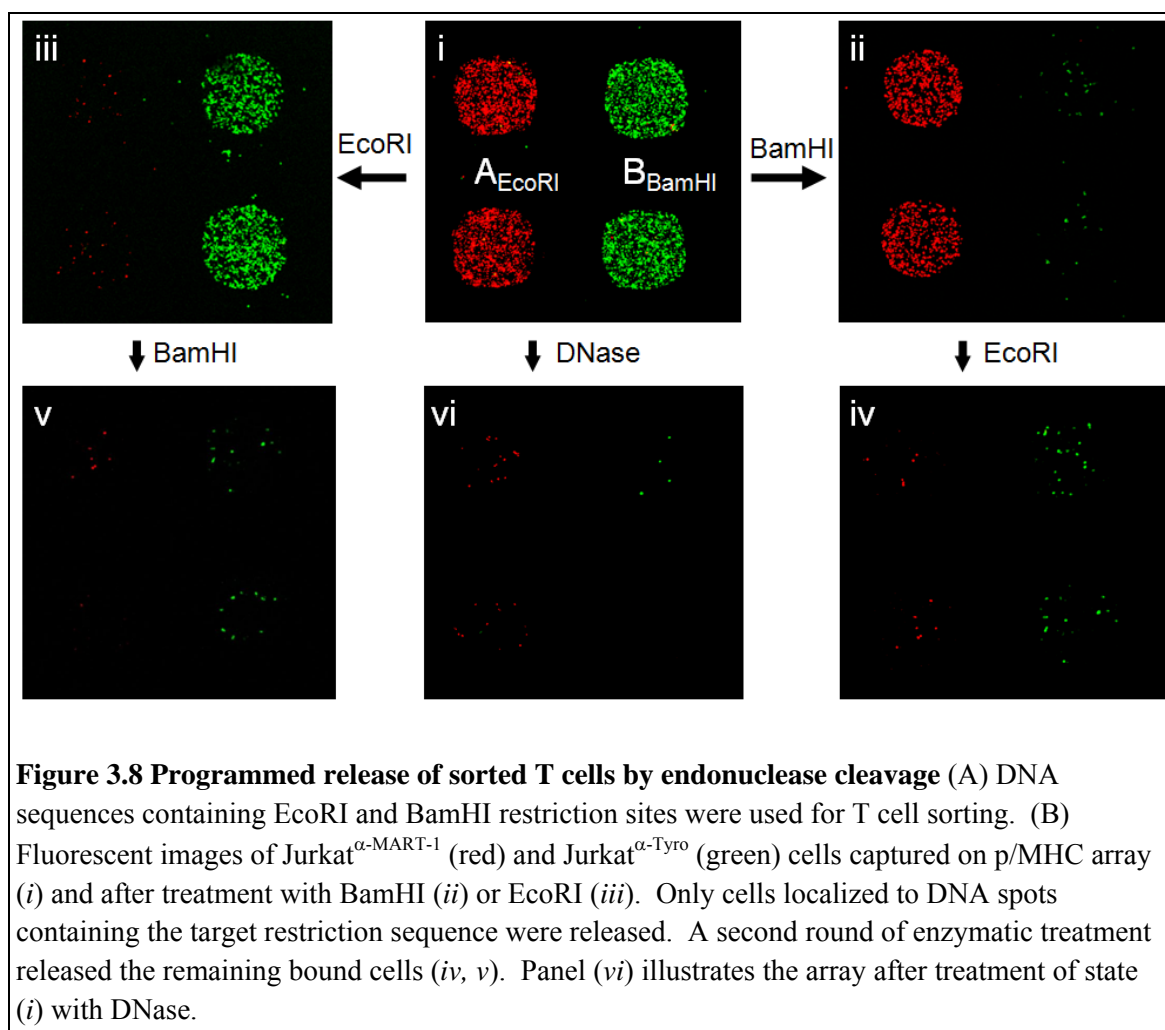
It should be noted, however, that the sensitivity of this approach cannot be increased without limiting scalability. Since spot diameters are required to be sufficiently large to detect a population at low frequency, this sets an upper bound on the number of distinct spots that can be patterned on a substrate. In the current instance, 600 μm spots are printed in 12 by 12 grids ($\sim 1 \text{ in}^2$), enabling the potential identification of 144 distinct antigen-specificities $\geq 0.1\%$ from 10^6 T cells (10^6 cells is typically required to cover a 1 in^2 region). In order to detect target populations below 0.1% without decreasing multiplexing, p/MHC-specific enrichment strategies (e.g. magnetic bead-based schemes (36)) can be implemented prior to cell sorting. Lastly, the recovery of this technique—defined as the total number of antigen-specific T cells captured as a fraction of the number of T cells applied to the array—is low relative to other sorting technologies like FACS and bead-based schemes. Typical T cell recovery for NACS is $\leq 20\%$ (37). In comparison, fluorescent-based sorting techniques like FACS have high recoveries, since

each stained T cell can be identified individually by the cytometer and sorted from the null population. The recovery (as well as sensitivity) of NACS will likely be improved by circulating T cells over the p/MHC array with agitation or with integrated microfluidic devices to allow T cells to sample the entire array.

3.3.4 Selective Release of Immobilized T cells with Restriction Endonucleases

Antigen-specific T cells immobilized onto glass are immediately available for secondary assays, since many such as immunohistochemistry (IHC), fluorescent in situ hybridization (FISH) and cytokine secretion assays (6, 8) are traditionally performed or are compatible with cells localized to a substrate. However, several other relevant assays, such as those designed to assess T cell phenotype or functional status like genomic/mRNA analysis or simply further culture for phenotypic enrichment would require a method for releasing the captured cells. Any release scheme should ideally be selective for given cell types. For NACS, we explored whether the DNA tethers could be selectively cleaved by exploiting the sequence specificity of restriction endonucleases. We integrated unique restriction sites to each DNA sequence employed for cell sorting, and found that the adhesion of different populations of antigen-specific T cells could, in fact, be independently controlled (**Figure 3.8**). Jurkat ^{α -MART-1} and Jurkat ^{α -Tyr} cells prestained with lipophilic dyes (red and green respectively) were sorted on an array printed with DNA sequences A_{EcoRI} and B_{BamHI} (**Figure 3.8i**). These oligonucleotides were modified by incorporating 6 bp restriction sites specific for endonucleases EcoRI and BamHI respectively. After T cell immobilization, the array was treated with BamHI which cleaved the B_{BamHI} spots and selectively released the bound Jurkat ^{α -Tyr} cells (**Figure 3.8ii**). Conversely, on a separate but identically cell sorted array, Jurkat ^{α -MART-1}

cells were released after treatment with EcoRI (**Figure 3.8iii**). A second round of enzymatic treatment with the complementary endonuclease (EcoRI to state *(ii)* or BamHI to state *(iii)*) removed the remaining adherent cells (*(iv, v)*). Alternatively all captured cells *(i)* could be released non-selectively in a single step with the addition of DNase *(vi)*.

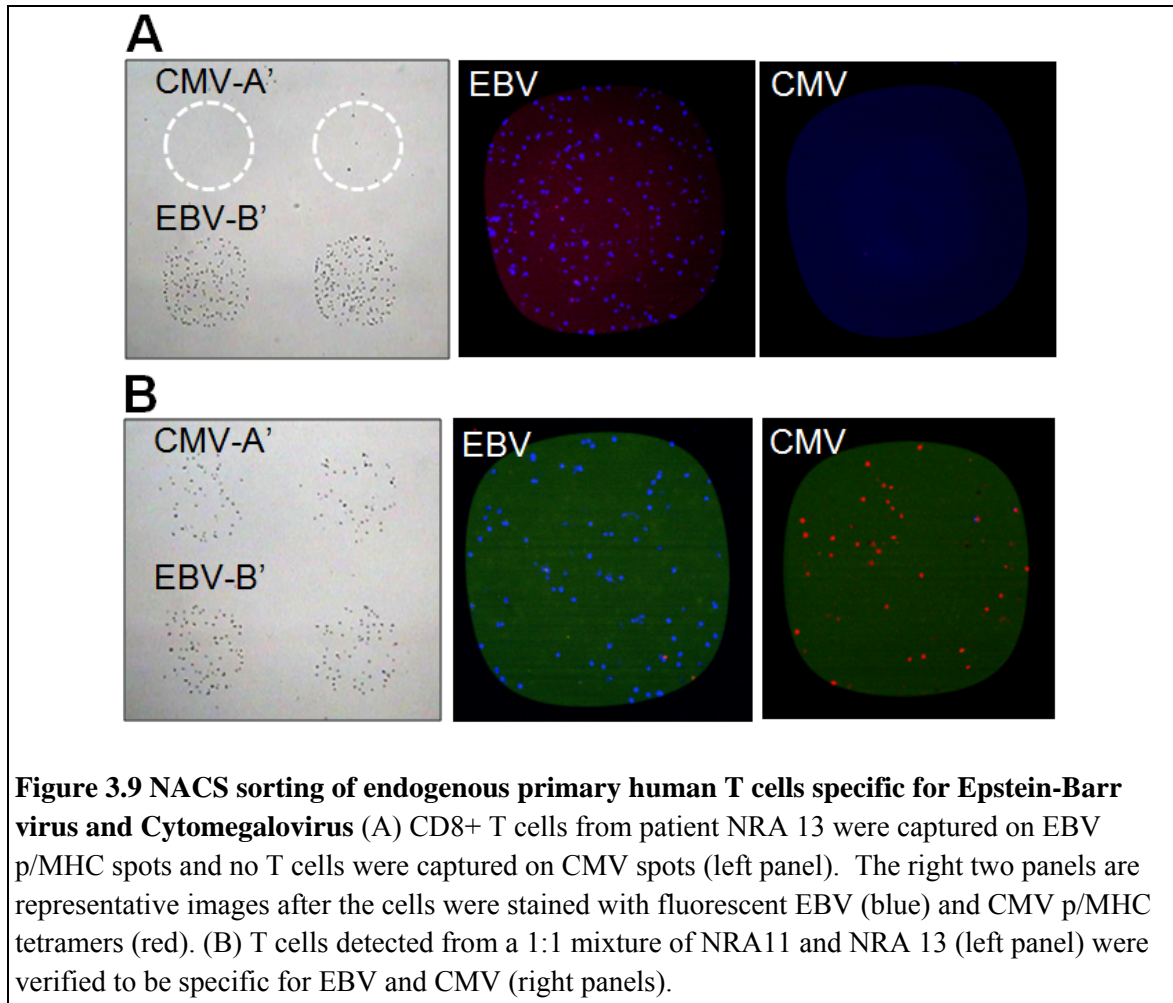


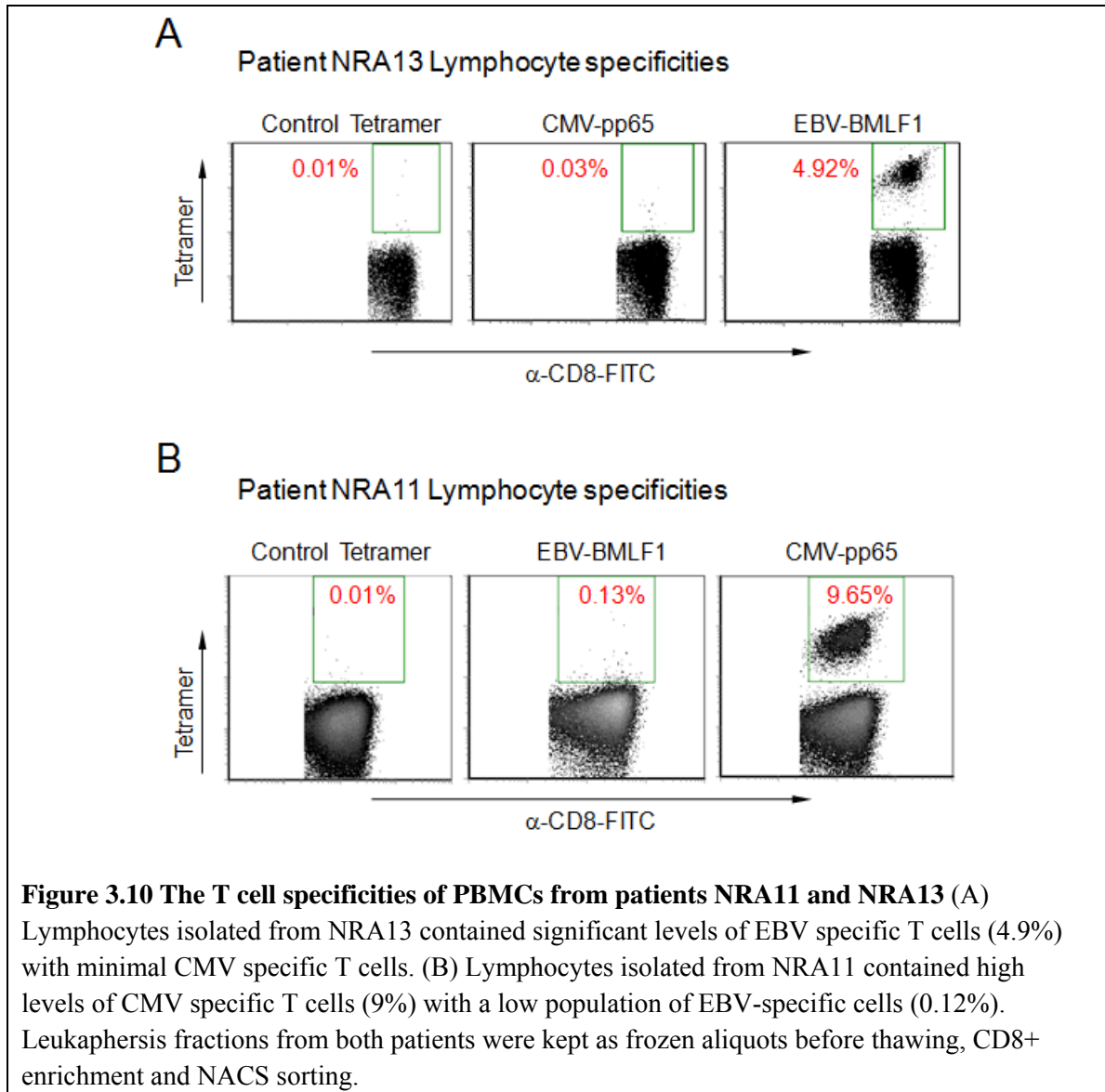
3.3.5 NACS sorting of endogenous primary human T cells

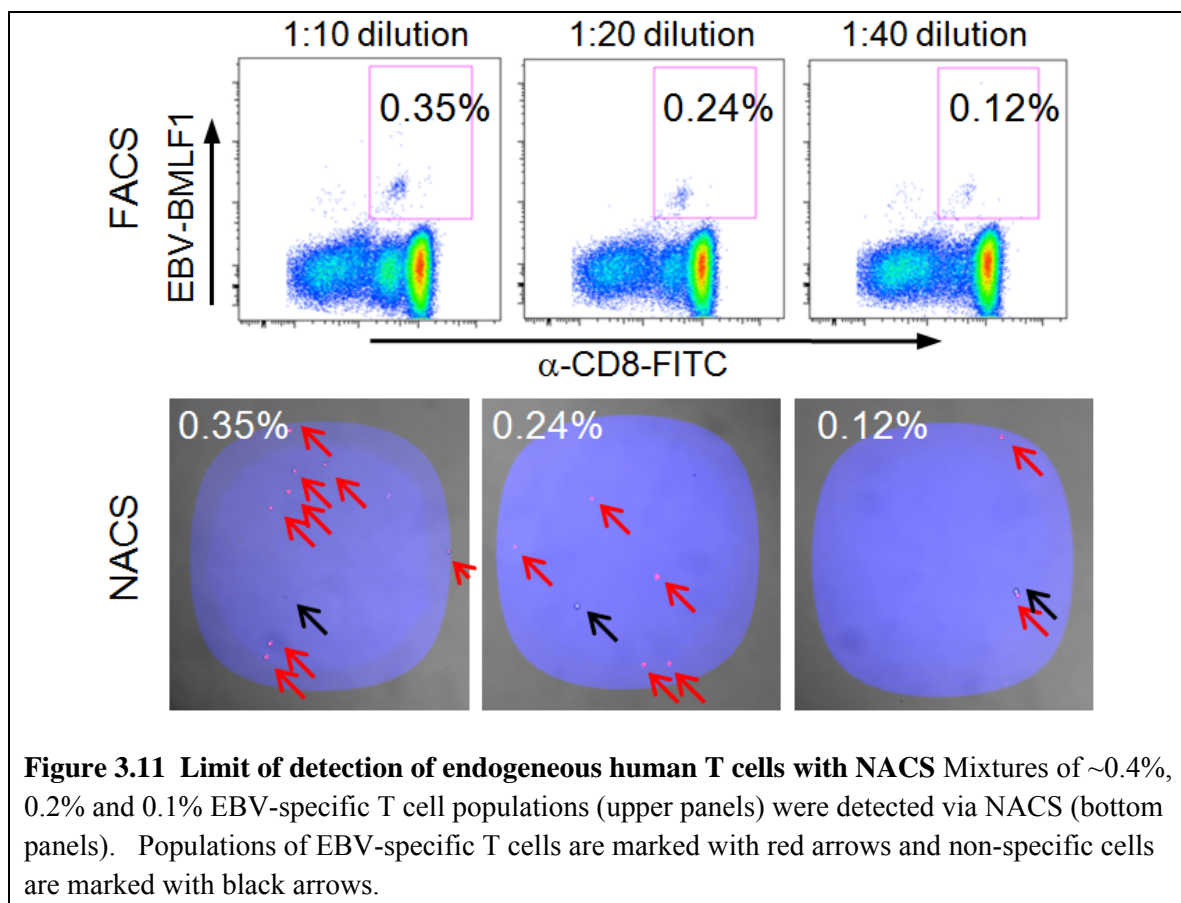
Detection of primary human T cells isolated from peripheral blood is generally more demanding than cultured cell lines because a single population of antigen-specific T cells is present within a large background of differing blood cells and of T cells expressing monoclonal and polyclonal TCRs of diverse specificities. In addition, these T cells would be expressing endogenous levels of TCR. We explored whether the same attributes of NACS that were found in the above examples would apply equally to endogenous primary human T cells. Frozen leukapheresis samples from patient NRA13 were CD8⁺ enriched and applied to a CMV and Epstein-barr virus (EBV BMLF1₂₅₉₋₂₆₇/HLA-A2.1) p/MHC array. T cells were captured only within the EBV regions only (**Figure 3.9A**). NRA13 CD8⁺ cells were verified by flow cytometry to be ~5% EBV-specific and ~0% CMV-specific (**Figure 3.10A**). The registry of the array was determined with the addition of A'-cy3 (red) and B'-cy5 (blue) conjugates.

For multiplexed detection, a 1:1 mixture of EBV-specific and CMV-specific CD8⁺ T cells was produced by combining NRA13 lymphocytes with CMV-specific T cells from patient NRA11 (**Figure 3.10B**). Following cell sorting and fluorescent p/MHC tetramer staining, the populations were complementary stained for the appropriate antigen-specificity (**Figure 3.9B**). The detection limit of antigen-specific T cells was evaluated from using serially diluted mixtures of EBV-specific T cells (~0.4%, 0.2%, and 0.1% by FACS) that were probed on an array. Isolated hits were resolved in frequencies as low as ~0.1% (**Figure 3.11**, red arrows). The number of unstained cells within the capture regions (black arrow) was constant throughout all dilutions (~1–2 cells/spot) and likely represents the level of background from non-specific interactions.

It should be noted that while we incorporated fluorescent p/MHC tetramer staining after T cell immobilization for illustrative purposes, the specificity of the captured cells could be determined solely from the registry of the array.







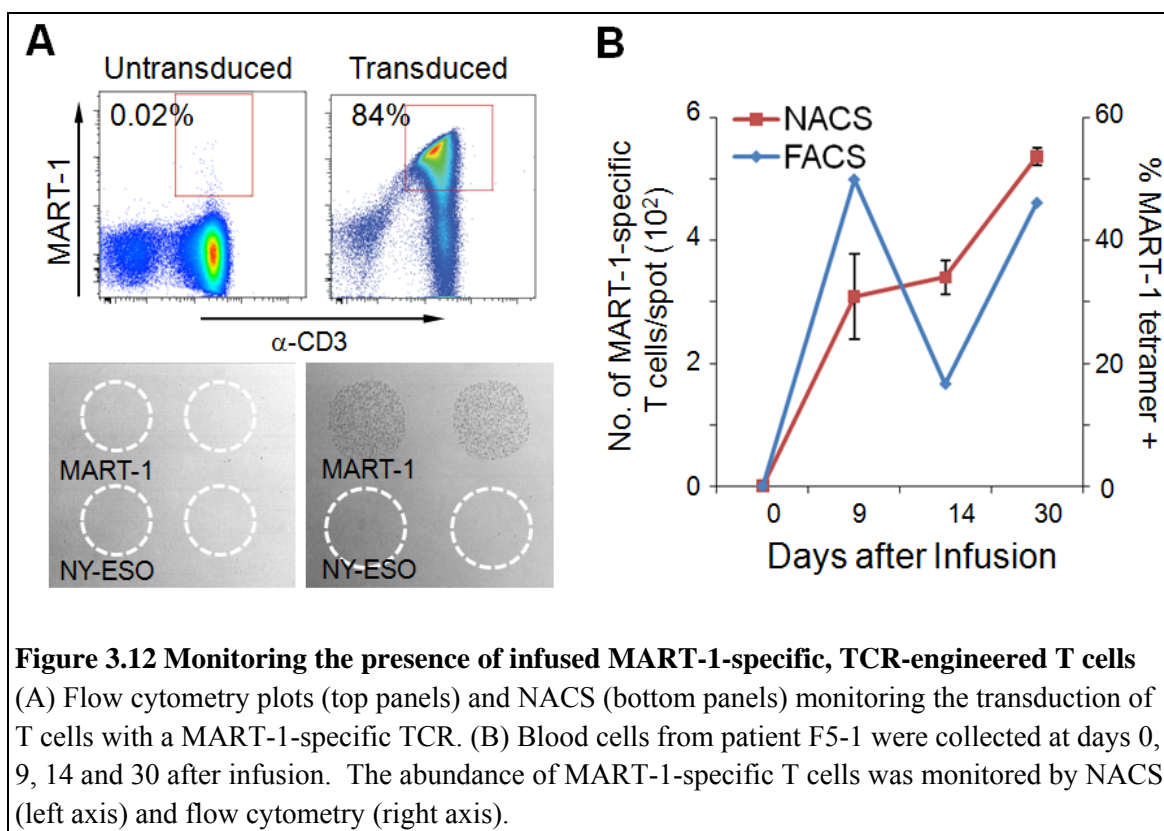
3.3.6 Persistence of MART-1 specific, TCR-engineered human T cells *in vivo*

One important potential application of NACS is to utilize the technique for monitoring cancer patients that are undergoing a particular type of immunotherapy that involves TCR engineering of peripheral blood mononuclear cells (PBMCs). This is an emerging clinical approach to rapidly generate large numbers of tumor antigen-specific T cells. In particular, a cancer patient's T cells are collected, genetically modified to express a TCR specific for a desired cancer antigen, and then they are introduced back into the patient as a cancer therapy. After re-infusion into the patient, the modified T cells can subsequently traffic to and engage with cancer cells, promoting tumor regression in a subset of patients with metastatic cancers. This type of directed cell

therapy is utilized primarily in patients with melanoma (skin cancer), but also for other cancers (38, 39). This approach is called adoptive cell transfer (ACT). We monitored the presence and abundance of TCR-engineered T cells in peripheral blood of a patient undergoing ACT. White blood cells were collected from patient F5-1 with metastatic melanoma. After in vitro expansion and TCR transduction, the cells were > 80% specific for the MART-1 p/MHC tetramer (**Figure 12A**). These cells were subsequently infused into patient F5-1 and the presence and persistence of MART-1-specific T cells in the peripheral blood was monitored by NACS at days 0 (prior to infusion), 9, 14 and 30 (**Figure 12B**). MART-1-specific T cells were not detectable in pre-infusion samples from the patient but they were detectable at all subsequent time points. This is represented as a gradual rise in the abundance of MART-1-specific T cells until day 30 (left axis). In comparison, the frequency of MART-1-specific T cells detected by flow cytometry spiked initially before decreasing and finally increasing by day 30 (right axis).

The abundance of TCR-engineered T cells, as measured by NACS, was generally correlated with parallel measurements using flow cytometry. The prospect of array-based T cell detection schemes for experimental cancer immuno-therapies such as ACT will likely increase as more cancer associated antigens are identified and targeted. For example, more than 50 different melanoma associated antigens have thus far been characterized (40, 41), and this means that more T cells types are likely to be employed for future therapies (39, 42, 43). However, the desire to probe larger sets of cancer associated antigens will be compounded by the amount of sample that can be practically collected from a patient. NACS appears to provide a feasible approach towards carrying

out the highly multiplexed cellular measurements that will eventually be required as ACT-like therapies move forward.



3.3.7 Homogeneous platform for cell sorting and functional analysis

Antigen-specific T cells that are sorted by NACS are immobilized to a solid surface and are immediately available for further studies. Traditional surface bound assays such as IHC, FISH and ELISPOT should integrate seamlessly with NACS. In addition, antigen-specific T cells have been shown to be activated upon binding to p/MHC arrays (6–8) and secrete various immunomodulatory cytokines. The cytokine secretion profiles of CD8⁺ T cells provide valuable information concerning the phenotype of the T cell (e.g. effector and anergic phenotypes can be differentiated by the

production of IFN- γ). Thus integrating on-chip cytokine measurements with antigen-specific T cell capture would greatly expand the diagnostic capability of NACS p/MHC tetramer arrays.

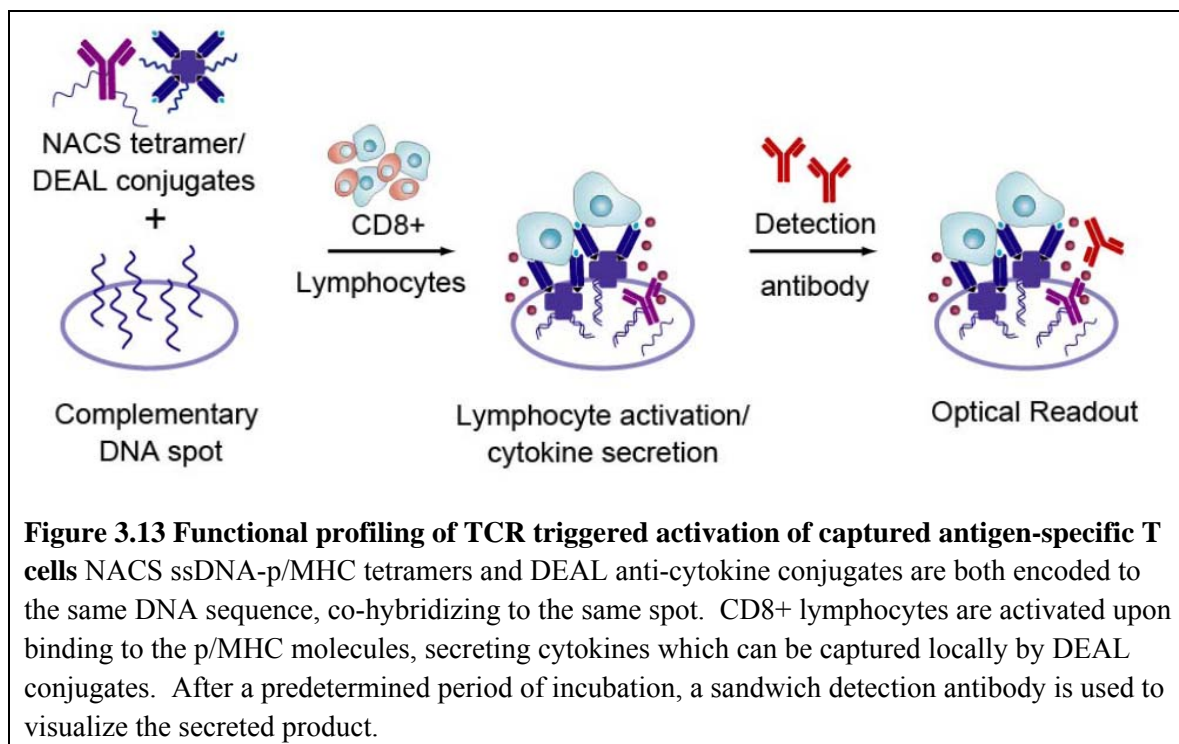


Figure 3.13 Functional profiling of TCR triggered activation of captured antigen-specific T cells NACS ssDNA-p/MHC tetramers and DEAL anti-cytokine conjugates are both encoded to the same DNA sequence, co-hybridizing to the same spot. CD8⁺ lymphocytes are activated upon binding to the p/MHC molecules, secreting cytokines which can be captured locally by DEAL conjugates. After a predetermined period of incubation, a sandwich detection antibody is used to visualize the secreted product.

We proceeded by integrating an ELISPOT-type sandwich assay with p/MHC NACS to detect cytokines produced by captured murine TCR transgenic splenocytes “on-the-spot” (**Figure 3.13**). Three murine anti-cytokine antibodies (IL-2, IFN- γ and TNF- α) were encoded with DNA strands A', B', and C' respectively. H-2K^b-OVA₂₅₇₋₂₆₄ ssDNA-p/MHC tetramers were encoded to all three strands. The ssDNA-p/MHC tetramers and antibody conjugates were pooled and assembled to a microarray printed with the complementary strands A, B and C. Murine OT1 lymphocytes (derived from TCR transgenic mice in which most splenocytes are specific for the model antigen OVA₂₅₇₋₂₆₄), were then seeded on the array. Following incubation periods of 2, 5, or 18 hours, pooled cytokine detection antibodies were added and the slide imaged by confocal

microscopy (**Figure 3.14A**). The inflammatory cytokine IFN- γ was detected at time points 5 and 18, manifest as discrete diffusive clusters (~ 50 – 100 μm in diameter at 5 hrs) that increased in average diameter temporally, attributable to molecular diffusion and sustained secretion. Examination of the vicinity of each burst showed that underlying each fluorescent cluster was a single cell while neighboring cells appeared to be non-responders (**Figure 3.14B**), suggestive that each IFN- γ burst was derived from a single cell. The number of IFN- γ clusters remained constant at ~ 3 between hours 5 and 18, indicating no increase in the number of activated T cells between those hours. No significant levels of murine IL-2 and TNF- α were detected at these time points.

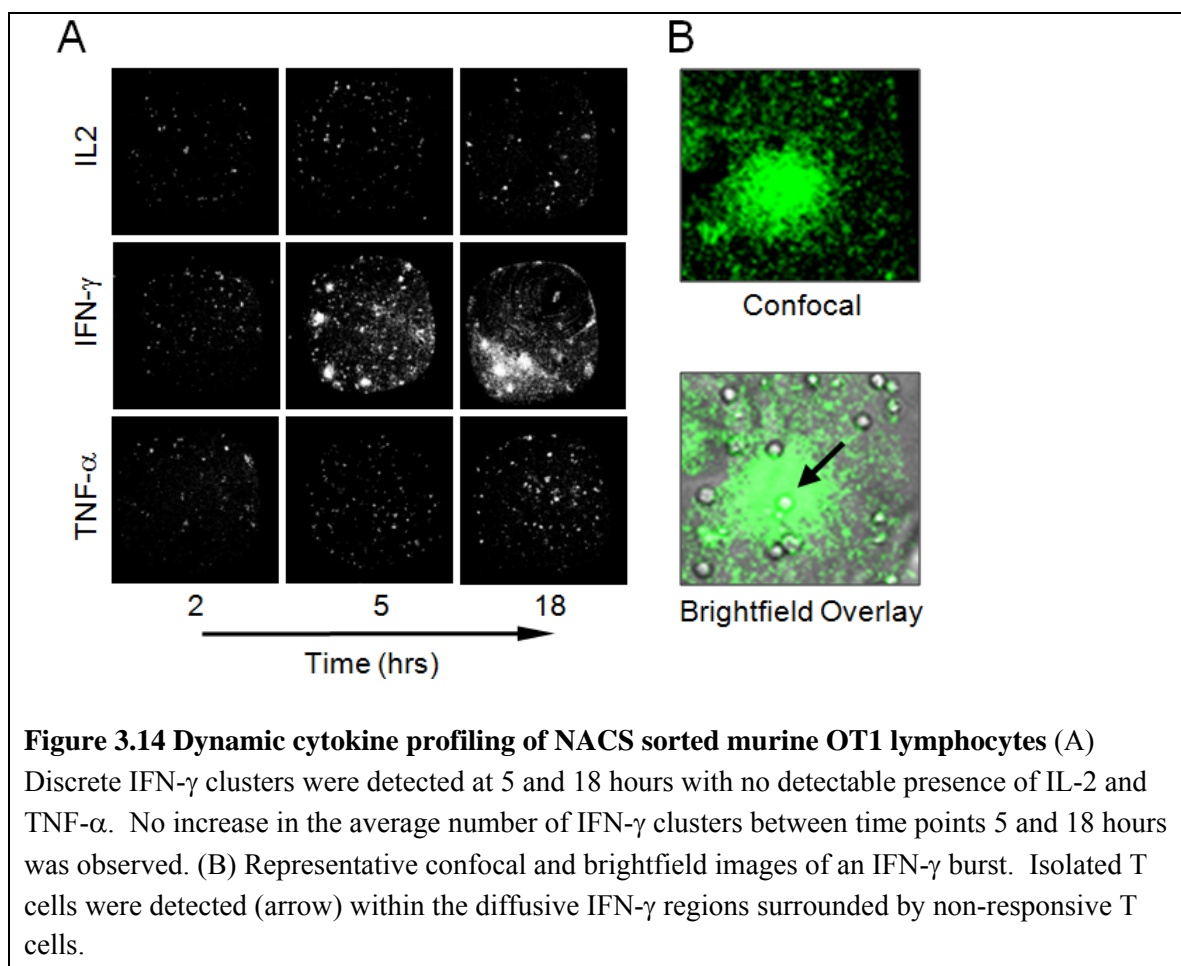


Figure 3.14 Dynamic cytokine profiling of NACS sorted murine OT1 lymphocytes (A)

Discrete IFN- γ clusters were detected at 5 and 18 hours with no detectable presence of IL-2 and TNF- α . No increase in the average number of IFN- γ clusters between time points 5 and 18 hours was observed. (B) Representative confocal and brightfield images of an IFN- γ burst. Isolated T cells were detected (arrow) within the diffusive IFN- γ regions surrounded by non-responsive T cells.

3.4 Conclusions

We have described a method for generating robust and modular p/MHC arrays for high efficiency T cell sorting. The inclusion of a larger set of orthogonal DNA sequences (20, 25) will enable the modular assembly of higher order p/MHC arrays for T cell screening experiments (e.g. one working set of DNA sequences can be used interchangeably to generate any combination of p/MHC arrays). This would find immediate utility in the field of TCR peptide epitope discovery where recently, novel antigen peptides were discovered via high-throughput CD8⁺ screening experiments utilizing multi-color flow cytometry in mice and humans (44, 45) (as many as 2,000 distinct p/MHC tetramers were prepared and tested). NACS arrays have the potential to streamline such experiments. Although traditional methods of producing single p/MHC monomers are time and labor intensive, recent reports using conditional peptide exchange technology enables the relatively straightforward construction of 1000 element p/MHC libraries rapidly (44–46). The integration of NACS with these peptide exchange technologies is a realistic option.

We have also demonstrated a number of advantages of the NACS platform. It significantly outperforms literature approaches that utilize surface-bound p/MHC tetramers to capture cells. It is simple and inexpensive to implement since cell sorting is performed on glass substrates prepared via traditional DNA printing technologies. In addition, sorted cells may be selectively released, which should permit for the deployment of a host of bioanalytical methods on NACS sorted cells. We envision that NACS will find uses beyond multiplexed sorting of T cells based on TCR specificity. The principal components of this platform—streptavidin-cysteine core and orthogonal

single stranded DNA sequences—were rationally developed to enable oriented coupling and spatial addressing. Thus this platform is amenable to any family of binding proteins or small molecule binders labeled with biotin. The increase in avidity of p/MHC tetramers over monomers as a consequence of the valency of SA should likewise extend to other capture agents, making it feasible to generate cellular arrays with probes ranging from high to moderate affinities like antibodies, aptamers or peptides.

3.5 References

1. Arstila, T.P.; Casrouge, A.; Baron, V.; Even, J.; Kanellopoulos, J.; Kourilsky, P. A Direct Estimate of the Human alpha beta T Cell Receptor Diversity. *Science* **1999**, *286*, 958–961.
2. Altman, J.D.; Moss, P.A.H.; Goulder, P.J. R.; Barouch, D.H.; McHeyzer-Williams, M.G.; Bell, J.I.; McMichael, A.J.; Davis, M.M. Phenotypic analysis of antigen-specific T lymphocytes. *Science* **1996**, *274*, 94–96.
3. Matsui, K.; Boniface, J.J.; Steffner, P.; Reay, P.A.; Davis, M.M. Kinetics of T-cell receptor binding to peptide/I-Ek complexes: correlation of the dissociation rate with T cell responsiveness. *Proc. Natl. Acad. Sci. USA* **1994**, *91*, 12862–12866.
4. McLaughlin, B.E.; Baumgarth, N.; Bigos, M.; Roederer, M.; DeRosa, S.C., Altman, J.D.; Nixon, D.F.; Ottinger, J.; Oxford, C.; Evans, T.G.; Asmuth, D.M. Nine-color flow cytometry for accurate measurement of T cell subsets and cytokine responses. Part I: Panel design by an empiric approach. *Cytometry A* **2008**, *73*, 400–410.
5. Chattopadhyay, P.K.; Price, D.A.; Harper, T.F.; Betts, M.R.; Yu, J.; Gostick, E.; Perfetto, S.P.; Goepfert, P.; Koup, R.A.; De Rosa, S.C.; Bruchez, M.P.; Roederer, M. Quantum dot semiconductor nanocrystals for immunophenotyping by polychromatic flow cytometry. *Nat. Med.* **2006**, *12*, 972–977.
6. Chen, D.S.; Soen, Y.; Stuge, T.B.; Lee, P.P.; Weber, J.S.; Brown, P.O.; Davis, M.M. Marked Differences in Human Melanoma Antigen-Specific T Cell Responsiveness after Vaccination Using a Functional Microarray. *PLoS Med.* **2005**, *2*, 1018–1030.
7. Soen, Y.; Chen, D.S.; Kraft, D.L.; Davis, M.M.; Brown, P.O. Detection and characterization of cellular immune responses using peptide-MHC microarrays. *PLoS Biol.* **2003**, *1*, 429–438.

8. Stone, J.D.; Demkowicz, W.E.; Stern, L.J. HLA-restricted epitope identification and detection of functional T cell responses by using MHC-peptide and costimulatory microarrays. *Proc. Natl. Acad. Sci. USA* **2005**, *102*, 3744–3749.
9. Deviren, G.; Gupta, K.; Paulaitis, M.E.; Schneck, J.P. Detection of antigen-specific T cells on p/MHC microarrays. *J. Mol. Recognit.* **2007**, *20*, 32–38.
10. Haab, B.B.; Dunham, M.J.; Brown, P.O. Protein microarrays for highly parallel detection and quantitation of specific proteins and antibodies in complex solutions. *Genome Biology* **2001**, *2*, 1–13.
11. Butler, J.E. ; Ni, L.; Brown, W.R.; Joshi, K.S.; Chang, J.; Rosenberg, B.; Voss Jr, E.W. The immunochemistry of sandwich ELISAs VI: Greater than 90% of monoclonal and 75% of polyclonal anti-fluorescyl capture antibodies (CAbs) are denatured by passive adsorption. *Mol. Immunol.* **1993**, *30*, 1165–1175.
12. Butler, J. E.; Ni, L.; Nessler, R.; Joshi, K.S.; Suter, M.; Rosenberg, B.; Chang, J.; Brown, W.R.; CantareroButler, L.A. The physical and functional behavior of capture antibodies adsorbed on polystyrene. *J Immunol. Methods*, **1992**, *150*, 77–90.
13. MacBeath, G.; Schreiber, S.L. Printing Proteins as Microarrays for High-Throughput Function Determination. *Science* **2000**, *289*, 1760–1763.
14. Lesaicherre, M. L.; Lue, Y.P.R.; Chen, G.Y.J.; Zhu, Q.; Yao, Q. Intein-Mediated Biotinylation of Proteins and Its Application in a Protein Microarray. *J. Am. Chem. Soc.* **2002**, *124*, 8768–8769.
15. Peluso, P.; Wilson, D.; Do, D.; Tran, H.; Venkatasubbaiah, M.; Quincy, D.; Heidecker, B.; Poindexter, K.; Tolani, N.; Phelan, M.; Witte, K.; Jung, L.; Wagner, P.; Nock, S. Optimizing antibody immobilization strategies for the construction of protein microarrays. *Anal. Biochem.* **2003**, *312*, 113–124.

16. Kwon, Y.; Han, Z.; Karatan, E.; Mrksich, M.; Kay, B. K. Antibody arrays prepared by cutinase-mediated immobilization on self-assembled monolayers. *Anal. Chem.* **2004**, *76*, 5713–5720.
17. Arenkov, P.; Kukhtin, A.; Gemmel, A.; Voloshchuk, S.; Chupeeva, V.; Mirzabekov, A. Protein microchips: use for immunoassay and enzymatic reactions. *Anal. Biochem.* **2000**, *278*, 123–131.
18. Kiyonaka, S.; Sada, K.; Yoshimura, I.; Shinkai, S.; Kato, N.; Hamachi, I. Semi-wet peptide/protein array using supramolecular hydrogel. *Nat. Mater.* **2004**, *3*, 58–64.
19. For example, the polyacrylamide surface employed by Davis and co-workers^{6,7} has been discontinued from the manufacturer (Perkin Elmer).
20. Bailey, R.C.; Kwong, G.A.; Radu, C.G.; Witte, O.N.; Heath, J.R. DNA-Encoded Antibody Libraries: A Unified Platform for Multiplexed Cell Sorting and Detection of Genes and Proteins. *J Am. Chem. Soc.* **2007**, *129*, 1959–1967.
21. Boozer, C.; Ladd, J.; Chen, S.F.; Jiang, S.T. DNA-directed protein immobilization for simultaneous detection of multiple analytes by surface plasmon resonance biosensor. *Anal. Chem.* **2006**, *78*, 1515–1519.
22. Niemeyer, C.M. Functional devices from DNA and proteins. *Nano Today* **2007**, *2*, 42–52.
23. Chandra, R.A.; Douglas, E.S.; Mathies, R.A.; Bertozzi, C.R.; Francis, M.B. Programmable cell adhesion encoded by DNA hybridization. *Angew. Chem. Int. Ed. Engl.* **2006** *45*, 896–901.
24. Hsiao, S.C.; Crow, A.K.; Lam, W.A.; Bertozzi, C.R.; Fletcher, D.A.; Francis, M.B. DNA-coated AFM cantilevers for the investigation of cell adhesion and the patterning of live cells. *Angew. Chem. Int. Ed. Engl.* **2008**, *47*, 8473–7.

25. Fan, R.; Vermesh, O.; Srivastava, A.; Yen, B.K.H.; Qin, L.; Ahmad, H.; Kwong, G.A.; Liu, C.C.; Gould, J.; Hood, L.; Heath, J.R. Integrated barcode chips for rapid, multiplexed analysis of proteins in microliter quantities of blood. *Nat. Biotechnol.* **2008**, *26*, 1373–1378
26. Sano, T.; Cantor, C.R. Expression of a cloned streptavidin gene in *Escherichia coli*. *Proc. Natl. Acad. Sci. USA* **1990**, *87*, 142–146.
27. Szymczak, A.L.; Workman, C.J.; Wang, Y.; Vignali, K.M.; Dilioglou, S.; Vanin, E.F.; Vignali, D.A.A. Correction of multi-gene deficiency in vivo using a single 'self-cleaving' 2A peptide-based retroviral vector. *Nat. Biotechnol.* **2004**, *22*, 589–594.
28. Garboczi, D.N.; Hung, D.T.; Wiley, D.C. HLA-A2-peptide complexes - refolding and crystallization of molecules expressed in *Escherichia coli* and complexed with single antigenic peptides. *Proc. Natl. Acad. Sci. USA* **1992**, *89*, 3429–3433.
29. Ramachandiran, V.; Grigoriev, V.; Lan, L.; Ravkov, E.; Mertens, S.A.; Altman, J.D. A robust method for production of MHC tetramers with small molecule fluorophores. *J. Immunol. Methods* **2007**, *319*, 13–20.
30. Cameron, T.O.; Cochran, J.R.; Yassine-Diab, B.; Sekaly, R.P.; Stern, L.J. Detection of Antigen-Specific CD4⁺ T Cells by HLA-DR1 Oligomers Is Dependent on the T Cell Activation State. *J. Immunol.* **2001**, *166*, 741–745.
31. Reznik, G.O.; Vajda, S.; Cantor, C.R.; Sano, T. A Streptavidin Mutant Useful for Directed Immobilization on Solid Surfaces. *Bioconj. Chem.* **2001**, *12*, 1000–1004.
32. Green, N.M. Spectrophotometric determination of biotin. *Methods Enzymol.* **1970**, *18*, 418–424.
33. Johnson, L.A.; Heemskerk, B.; Powell, D.J.; Cohen, C.J.; Morgan, R.A.; Dudley, M.E.; Robbins, P.F.; Rosenberg, S.A. Gene Transfer of Tumor-Reactive TCR Confers Both High Avidity and Tumor Reactivity to Nonreactive Peripheral

- Blood Mononuclear Cells and Tumor-Infiltrating Lymphocytes. *J. Immunol.* **2006**, *177*, 6548–6559.
34. Nishimura, M.I.; Avichezer, D.; Custer, M.C.; Lee, C.S.; Chen, C.; Parkhurst, M.R.; Diamond, R.A.; Robbins, P.F.; Schwartzentruber, D.J.; Rosenberg, S.A. MHC Class I-restricted Recognition of a Melanoma Antigen by a Human CD4+ Tumor Infiltrating Lymphocyte. *Cancer Res.* **1999**, *59*, 6230–6238.
 35. Wargo, J.A.; Robbins, P.F.; Li, Y.; Zhao, Y.; El-Gamil, M.; Caragacianu, D.; Zheng, Z.; Hong, J.A.; Downey, S.; Schrump, D.S.; Rosenberg, S.A.; Morgan, R.A. Recognition of NY-ESO-1+ tumor cells by engineered lymphocytes is enhanced by improved vector design and epigenetic modulation of tumor antigen expression. *Cancer Immunol. Immunother.* **2009**, *58*, 383–394.
 36. Moon, J.J.; Chu, H.H.; Pepper, M.; McSorley, S.J.; Jameson, S.C.; Kedl, R.M.; Jenkins, M.K. Naive CD4(+) T cell frequency varies for different epitopes and predicts repertoire diversity and response magnitude. *Immunity* **2007**, *27*, 203–213.
 37. For a typical homogeneous sorting experiment, 10^6 T cells are applied to an array containing 144 spots. Each spot can bind to $\sim 1486 \pm 62$ T cells. The recovery, R, is calculated as $R = 100\% \times (144 \times 1486)/10^6 \approx 20\%$. The recovery is valid even with heterogeneous samples (e.g. 1:1 mixture of two antigen-specific T cell populations) when the entire array is used to sort a single target population ($R = 100\% \times (144 \text{ spots} \times 661)/(5 \times 10^5) \approx 20\%$). For multiplexed experiments, R is proportional to the fraction of the 144 spots dedicated for cell capture. For example, sorting 2 populations from a 1:1 mixture, $R = 100\% \times (72 \text{ spots} \times 661)/(5 \times 10^5) \approx 10\%$.
 38. Schumacher, T.N. T-cell-receptor gene therapy. *Nat. Rev. Immunol.* **2002**, *2*, 512–519.
 39. Morgan, R.A.; Dudley, M.E.; Wunderlich, J.R.; Hughes, M.S.; Yang, J.C.; Sherry, R.M.; Royal, R.E.; Topalian, S.L.; Kammula, U.S.; Restifo, N.P.; et al.

- Cancer Regression in Patients After Transfer of Genetically Engineered Lymphocytes. *Science* **2006**, *314*, 126–129.
40. Rosenberg, S.A. A New Era for Cancer Immunotherapy Based on the Genes that Encode Cancer Antigens. *Immunity* **1999**, *10*, 281–287.
 41. Rosenberg, S.A. Progress in human tumour immunology and immunotherapy. *Nature* **2001**, *411*, 380–384.
 42. Dudley M.E.; et al. Cancer Regression and Autoimmunity in Patients After Clonal Repopulation with Antitumor Lymphocytes. *Science* **2002**, *298*, 850–854.
 43. Hunder, N.N.; Wallen, H.; Cao, J.; Hendricks, D.W.; Reilly, J.Z.; Rodmyre, R.; Jungbluth, A.; Gnjjatic, S.; Thompson, J.A.; Yee, C. Treatment of Metastatic Melanoma with Autologous CD4+ T Cells against NY-ESO-1. *N. Engl. J. Med.* **2008**, *358*, 2698–2703.
 44. Toebes, M.; Coccoris, M.; Bins, A.; Rodenko, B.; Gomez, R.; Nieuwkoop, N.J.; van de Kastele, W.; Rimmelzwaan, G.F.; Haanen, J.; Ovaas, H.; Schumacher, T.N. Design and use of conditional MHC class I ligands. *Nat. Med.* **2006**, *12*, 246–251.
 45. Grotenbreg, G.M.; Roan, N.R.; Guillen, E.; Meijers, R.; Wang, J.; Bell, G.W.; Starnbach, M.N.; Ploegh, H.L. Discovery of CD8+ T cell epitopes in *Chlamydia trachomatis* infection through use of caged class I MHC tetramers. *Proc. Natl. Acad. Sci. USA* **2008**, *105*, 3831–3836.
 46. Bakker, A.H.; Hoppes, R.; Linnemann, C.; Toebes, M.; Rodenko, B.; Berkers, C.R.; Hadrup, S.R.; van Esch, W.J.; Heemskerk, M.H.; Ovaas, H.; Schumacher, T.N. Conditional MHC class I ligands and peptide exchange technology for the human MHC gene products HLA-A1, -A3, -A11, and -B7. *Proc. Natl. Acad. Sci. USA* **2008**, *105*, 3825–3830.

3.6 Appendix A: Protein Sequences

Core streptavidin + Cys in pET-3a vector (NdeI/BamHI)

NdeI

1 CATATGGGCA TCACCGGCAC CTGGTACAAC CAGCTCGGCT CGACCTTCAT
H M G I T G T W Y N Q L G S T F I

51 CGTGACCGCG GGCGCCGACG GCGCCCTGAC CGGAACCTAC GAGTCGGCCG
V T A G A D G A L T G T Y E S A V

101 TCGGCAACGC CGAGAGCCGC TACGTCCTGA CCGGTCGTTA CGACAGCGCC
G N A E S R Y V L T G R Y D S A

151 CCGGCCACCG ACGGCAGCGG CACCGCCCTC GGTTGGACGG TGGCCTGGAA
P A T D G S G T A L G W T V A W K

201 GAATAACTAC CGCAACGCCC ACTCCGCGAC CACGTGGAGC GGCCAGTACG
N N Y R N A H S A T T W S G Q Y V

251 TCGGCGGGCG CGAGGCGAGG ATCAACACCC AGTGGCTGCT GACCTCCGGC
G G A E A R I N T Q W L L T S G

301 ACCACCGAGG CCAACGCCTG GAAGTCCACG CTGGTCGGCC ACGACACCTT
T T E A N A W K S T L V G H D T F

BamHI

351 CACCAAGGTG GGTGGTTCTG GTTGCCCCTAG GGATCC
T K V G G S G C P *

Human β_2m in pET-3a vector NdeI/BamHI

NdeI

1 CATATGATCC AGCGTACTCC AAAGATTCAG GTTTACTCAC GTCATCCAGC
H M I Q R T P K I Q V Y S R H P A

51 AGAGAATGGA AAGTCAAATT TCCTGAATTG CTATGTGTCT GGGTTTCATC
E N G K S N F L N C Y V S G F H P

101 CATCCGACAT TGAAGTTGAC TTAAGTGAAGA ATGGAGAGAG AATTGAAAAA
S D I E V D L L K N G E R I E K

151 GTGGAGCATT CAGACTTGTC TTTCAGCAAG GACTGGTCTT TCTATCTCTT
V E H S D L S F S K D W S F Y L L

201 GTATTATACT GAATTCACCC CCACTGAAAA AGATGAGTAT GCCTGCCGTG
Y Y T E F T P T E K D E Y A C R V

251 TGAACCACGT GACTTTGTCA CAGCCCAAGA TAGTTAAGTG GGATCGAGAC
 N H V T L S Q P K I V K W D R D

BamHI

301 ATGTAA GGATCC
 M *

Human HLA-A2.1 (biotin tag)

1 ATGGGCTCTC ACTCCATGAG GTATTTCTTC ACATCCGTGT CCCGGCCCCG
 M G S H S M R Y F F T S V S R P G

51 CCGCGGGGAG CCCCCTTCA TCGCAGTGGG CTACGTGGAC GACACGCAGT
 R G E P R F I A V G Y V D D T Q F

101 TCGTGCGGTT CGACAGCGAC GCCGCGAGCC AGAGGATGGA GCCGCGGGCG
 V R F D S D A A S Q R M E P R A

151 CCGTGGATAG AGCAGGAGGG TCCGGAGTAT TGGGACGGGG AGACACGGAA
 P W I E Q E G P E Y W D G E T R K

201 AGTGAAGGCC CACTCACAGA CTCACCGAGT GGACCTGGGG ACCCTGCGCG
 V K A H S Q T H R V D L G T L R G

251 GCTACTACAA CCAGAGCGAG GCCGGTTCTC ACACCGTCCA GAGGATGTAT
 Y Y N Q S E A G S H T V Q R M Y

301 GGCTGCGACG TGGGGTCGGA CTGGCGCTTC CTCCGCGGGT ACCACCAGTA
 G C D V G S D W R F L R G Y H Q Y

351 CGCCTACGAC GGCAAGGATT ACATCGCCCT GAAAGAGGAC CTGCGCTCTT
 A Y D G K D Y I A L K E D L R S W

401 GGACCGCGGC GGACATGGCA GCTCAGACCA CCAAGCACAA GTGGGAGGCG
 T A A D M A A Q T T K H K W E A

451 GCCCATGTGG CGGAGCAGTT GAGAGCCTAC CTGGAGGGCA CGTGCGTGGA
 A H V A E Q L R A Y L E G T C V E

501 GTGGCTCCGC AGATACCTGG AGAACGGGAA GGAGACGCTG CAGCGCACGG
 W L R R Y L E N G K E T L Q R T D

551 ACGCCCCAA AACGCATATG ACTCACCACG CTGTCTCTGA CCATGAAGCC
 A P K T H M T H H A V S D H E A

601 ACCCTGAGGT GCTGGGCCCT GAGCTTCTAC CCTGCGGAGA TCACACTGAC
 T L R C W A L S F Y P A E I T L T

651 CTGGCAGCGG GATGGGGAGG ACCAGACCCA GGACACGGAG CTCGTGGAGA

W Q R D G E D Q T Q D T E L V E T
 701 CCAGGCCTGC AGGGGATGGA ACCTTCCAGA AGTGGGCGGC TGTGGTGGTG
 R P A G D G T F Q K W A A V V V
 751 CCTTCTGGAC AGGAGCAGAG ATACACCTGC CATGTGCAGC ATGAGGGTTT
 P S G Q E Q R Y T C H V Q H E G L
 801 GCCCAAGCCC CTCACCGGAT CCGGTGGTTC CGGTGGTTCC GCGGGTGGTG
 P K P L T G S G G S G G S A G G G
 851 GTTTGAACGA CATCTTCGAA GCTCAGAAAA TCGAATGGCA CTAA
 L N D I F E A Q K I E W H *

BirA ligase biotin sequence: GGGLNDIFEAQKIEWH

Murine β_2m

1 ATGATCCAGA AAACCCCTCA AATTCAAGTA TACTCACGCC ACCCACCGBA
 M I Q K T P Q I Q V Y S R H P P E
 51 GAATGGGAAG CCGAACATAC TGAACTGCTA CGTAACACAG TTCCACCCGC
 N G K P N I L N C Y V T Q F H P P
 101 CTCACATTGA AATCCAAATG CTGAAGAACG GGAAAAAAT TCCTAAAGTA
 H I E I Q M L K N G K K I P K V
 151 GAGATGTCAG ATATGTCCTT CAGCAAGGAC TGGTCTTTCT ATATCCTGGC
 E M S D M S F S K D W S F Y I L A
 201 TCACACTGAA TTCACCCCCA CTGAGACTGA TACATACGCC TGCAGAGTTA
 H T E F T P T E T D T Y A C R V K
 251 AGCATGACAG TATGGCCGAG CCCAAGACCG TCTACTGGGA TCGAGACATG
 H D S M A E P K T V Y W D R D M
 301 TGA
 *

Murine Kb (biotin tag)

NdeI
 1 CATATGGGTC CACTCTCTCT GCGCTATTTT CTTACGGCTG TTAGCCGTCC
 H M G P H S L R Y F V T A V S R P
 51 GGGTCTGGGT GAGCCGCGCT ACATGGAAGT CGGTTACGTC GACGACACCG

G L G E P R Y M E V G Y V D D T E
 101 AATTCGTGCG TTTCGACAGC GACGCGGAGA ACCCGCGTTA TGAGCCGCGT
 F V R F D S D A E N P R Y E P R
 151 GCGCGTTGGA TGGAGCAGGA AGGTCCGGAG TACTGGGAGC GTGAAACGCA
 A R W M E Q E G P E Y W E R E T Q
 201 AAAGCGAAG GGCAATGAAC AGAGCTTTCG TGTTGATCTG CGCACTCTGC
 K A K G N E Q S F R V D L R T L L
 251 TGGGTTACTA CAACCAGAGC AAAGGTGGCA GCCATAACCAT TCAGGTGATT
 G Y Y N Q S K G G S H T I Q V I
 301 AGCGGTTGTG AAGTCGGCTC TGATGGCCGC CTGTTGCGCG GTTATCAGCA
 S G C E V G S D G R L L R G Y Q Q
 351 ATATGCATAC GACGTTGCG ACTACATTGC GCTGAATGAA GATCTGAAAA
 Y A Y D G C D Y I A L N E D L K T
 401 CGTGGACTGC GGCGGACATG GCCGCACTGA TTACCAAACA CAAGTGGGAG
 W T A A D M A A L I T K H K W E
 451 CAAGCGGGCG AAGCCGAGCG CCTGCGTGCG TATCTGGAAG GCACCTGTGT
 Q A G E A E R L R A Y L E G T C V
 501 GGAATGGCTG CGCCGCTATC TGAAGAATGG CAATGCCACG TTGCTGCGTA
 E W L R R Y L K N G N A T L L R T
 551 CGGATTCCCC GAAAGCGCAC GTGACGCACC ATAGCCGTCC TGAGGATAAA
 D S P K A H V T H H S R P E D K
 601 GTTACCCTGC GTTGCTGGGC ACTGGGCTTT TACCCGGCAG ATATCACCTT
 V T L R C W A L G F Y P A D I T L
 651 GACGTGGCAA CTGAATGGTG AAGAGCTGAT TCAGGATATG GAACTGGTGG
 T W Q L N G E E L I Q D M E L V E
 701 ARACTCGTCC GGCTGGCGAC GGTACCTTCC AGAAATGGGC ATCGGTTGTC
 T R P A G D G T F Q K W A S V V
 751 GTCCCTCTGG GTAAAGAGCA ATACTATAACC TGCCACGTTT ACCACCAAGG
 V P L G K E Q Y Y T C H V Y H Q G
 801 TCTGCCGGAG CCGCTGACCT TCGGTTGGGA GCCACCGCCG AGCACCGGCA
 L P E P L T L R W E P P P S T G S
 851 GCGGTGGTAG CGGCGGTTCC GCGGGTGGCG GTCTGAACGA CATCTTTGAG
 G G S G G S A G G G L N D I F E
 BamHI
 901 GCCCAGAAGA TCGAGTGGCA TTAAGGATCC

A Q K I E W H *

BirA ligase biotin sequence: GGGLNDIFEAQKIEWH

Murine Db (biotin tag)

1 ATGGGCCAC ACTCGATGCG GTATTTTCGAG ACCGCCGTGT CCCGGCCCCG
M G P H S M R Y F E T A V S R P G

51 CCTCGAGGAG CCCCGGTACA TCTCTGTCGG CTATGTGGAC AACAAAGGAGT
L E E P R Y I S V G Y V D N K E F

101 TCGTGCGCTT CGACAGCGAC GCGGAGAATC CGAGATATGA GCCGCGGGCG
V R F D S D A E N P R Y E P R A

151 CCGTGGATGG AGCAGGAGGG GCCGGAGTAT TGGGAGCGGG AAACACAGAA
P W M E Q E G P E Y W E R E T Q K

201 AGCCAAGGGC CAAGAGCAGT GGTTCGAGT GAGCCTGAGG AACCTGCTCG
A K G Q E Q W F R V S L R N L L G

251 GCTACTACAA CCAGAGCGCG GCGGCTCTC ACACACTCCA GCAGATGTCT
Y Y N Q S A G G S H T L Q Q M S

301 GGCTGTGACT TGGGGTCGGA CTGGCGCCTC CTCCGCGGGT ACCTGCAGTT
G C D L G S D W R L L R G Y L Q F

351 CGCCTATGAA GGCCGCGATT ACATCGCCCT GAACGAAGAC CTGAAAACGT
A Y E G R D Y I A L N E D L K T W

401 GGACGGCGGC GGACATGGCG GCGCAGATCA CCCGACGCAA GTGGGAGCAG
T A A D M A A Q I T R R K W E Q

451 AGTGGTGCTG CAGAGCATT CAAGGCCTAC CTGGAGGGCG AGTGCGTGGA
S G A A E H Y K A Y L E G E C V E

501 GTGGCTCCAC AGATACCTGA AGAACGGGAA CGCGACGCTG CTGCGCACAG
W L H R Y L K N G N A T L L R T D

551 ATTCCCCAAA GGCACATGTG ACCCATCACC CCAGATCTAA AGGTGAAGTC
S P K A H V T H H P R S K G E V

601 ACCCTGAGGT GCTGGGCCCT GGGCTTCTAC CCTGCTGACA TCACCCTGAC
T L R C W A L G F Y P A D I T L T

651 CTGGCAGTTG AATGGGGAGG AGCTGACCCA GGACATGGAG CTTGTGGAGA
W Q L N G E E L T Q D M E L V E T

701 CCAGGCCTGC AGGGGATGGA ACCTTCCAGA AGTGGGCATC TGTGGTGGTG
R P A G D G T F Q K W A S V V V

751 CCTCTTGGGA AGGAGCAGAA TTACACATGC CGTGTGTACC ATGAGGGGCT
P L G K E Q N Y T C R V Y H E G L

801 GCCTGAGCCC CTCACCCTGA GATGGGAGCC TCCTCCATCC ACTGGATCCG
P E P L T L R W E P P P S T G S G

851 GTGGTTCCGG TGGTTCCGCG GGTGGTGGTT TGAACGACAT CTTCGAAGCT
G S G G S A G G G L N D I F E A

901 CAGAAAATCG AATGGCACTA A
Q K I E W H *

3.7 Appendix B: Chromatography

3.7.1 Iminobiotin Purification of SAC

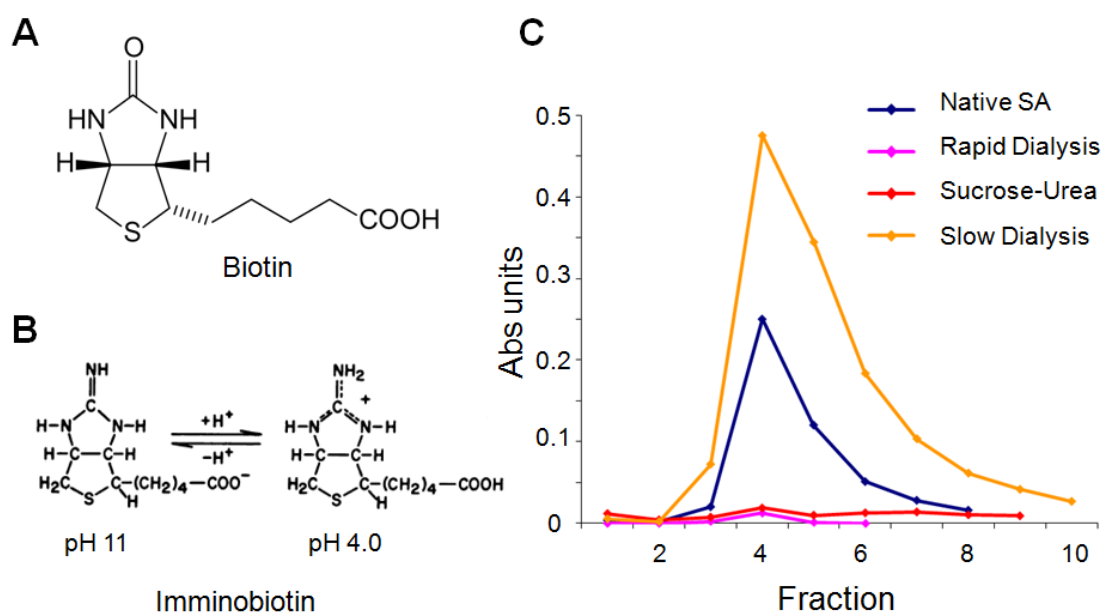
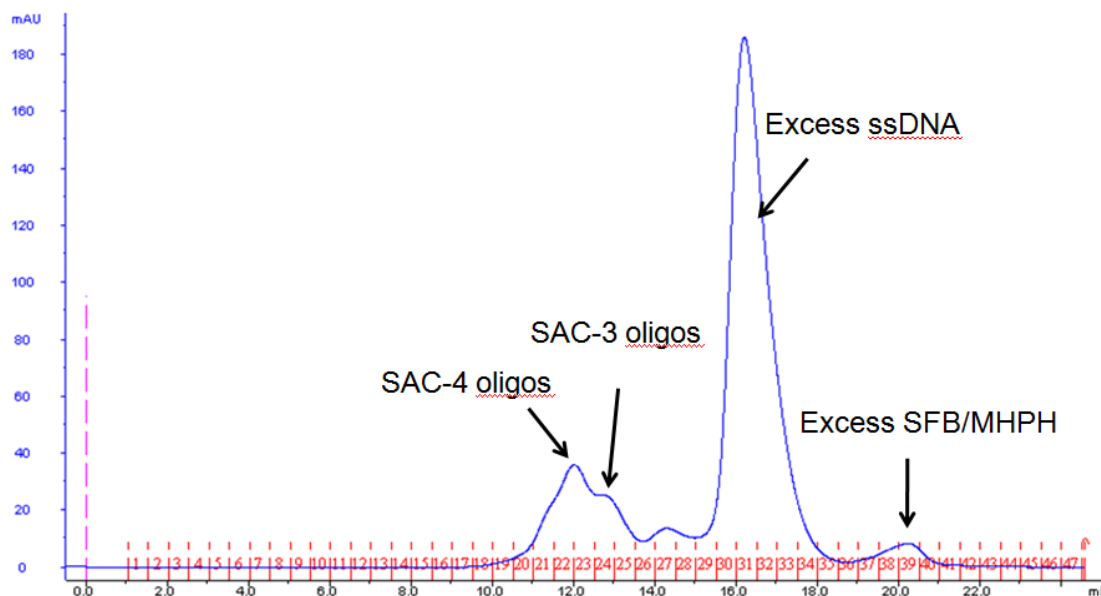


Figure 3.15 SAC purification with an iminobiotin agarose support column. (A) The structure of biotin. (B) Iminobiotin, the structural analog of biotin, has two distinct states; (1) a neutral, high affinity SAC binding state at pH 11 and a cationic state, low affinity SAC binding state at pH 4. (C) Elution profile of SA compared to SAC refolded in various buffers.

3.7.2 FPLC of SAC-ssDNA conjugates



*0.5ml/min isocratic flow of PBS

Figure 3.16 Fast protein liquid chromatography of ssDNA-SAC conjugates. A typical successful conjugation reaction will yield three distinct peaks, corresponding to the ssDNA-SAC conjugates, excess unreacted ssDNA, and excess small molecules. It is possible to resolve shoulders in the ssDNA-SAC peak, corresponding to extent of ssDNA modification.